
ANALYSIS AND OPTIMISATION OF BELLMAN RESIDUAL ERRORS WITH NEURAL FUNCTION APPROXIMATION

A PREPRINT

Martin Gottwald ^{*}
 martin.gottwald@tum.de

Sven Grounauer ^{*}
 sven.gronauer@tum.de

Hao Shen [†]
 shen@fortiss.org

Klaus Diepold ^{*}
 kldi@tum.de

October 9, 2021

ABSTRACT

Recent development of Deep Reinforcement Learning has demonstrated superior performance of neural networks in solving challenging problems with large or even continuous state spaces. One specific approach is to deploy neural networks to approximate value functions by minimising the Mean Squared Bellman Error function. Despite great successes of Deep Reinforcement Learning, development of reliable and efficient numerical algorithms to minimise the Bellman Error is still of great scientific interest and practical demand. Such a challenge is partially due to the underlying optimisation problem being highly non-convex or using incorrect gradient information as done in Semi-Gradient algorithms. In this work, we analyse the Mean Squared Bellman Error from a smooth optimisation perspective combined with a Residual Gradient formulation. Our contribution is two-fold.

First, we analyse critical points of the error function and provide technical insights on the optimisation procure and design choices for neural networks. When the existence of global minima is assumed and the objective fulfils certain conditions we can eliminate suboptimal local minima when using over-parametrised neural networks. We can construct an efficient Approximate Newton's algorithm based on our analysis and confirm theoretical properties of this algorithm such as being locally quadratically convergent to a global minimum numerically.

Second, we demonstrate feasibility and generalisation capabilities of the proposed algorithm empirically using continuous control problems and provide a numerical verification of our critical point analysis. We outline the short coming of Semi-Gradients. To benefit from an approximate Newton's algorithm complete derivatives of the Mean Squared Bellman error must be considered during training.

Keywords MSBE · Residual Gradient · Critical Point Analysis · Second Order Optimisation · Dynamic Programming

1 Introduction

Reinforcement Learning (RL), or more general *Dynamic Programming* (DP), is a general purpose framework to solve sequential decision making or optimal control problems. Those frameworks use *Value Function Approximation* (VFA) as an important and effective instrument to handle large or even infinite state spaces [Bertsekas, 2012, Sutton and Barto, 2020]. VFA methods can be categorised in two groups, *linear* and *non-linear*. Various efficient *Linear Value Function Approximation* (LVFA) algorithms have been developed and analysed in the field, e.g. [Nedić and Bertsekas, 2003, Bertsekas et al., 2004, Parr et al., 2008, Geist and Pietquin, 2013]. Despite their significant simplicity and convergence stability, the performance of LVFA methods depends heavily on construction and selection of linear features, which is a time consuming and hardly scalable process [Parr et al., 2007, Böhmer et al., 2013]. Therefore, recent research efforts have focused more on *Non-Linear Value Function Approximation* (NL-VFA) methods.

^{*}Chair for Data Processing, Technical University of Munich, Arcisstr. 21, 80333 Munich, Germany

[†]fortiss, Forschungsinstitut des Freistaats Bayern, Guerickestr. 25, 80805 Munich, Germany

As a popular non-linear mechanism, kernel tricks have been successfully adopted to VFA, and demonstrated their convincing performance in various applications [Xu et al., 2007, Taylor and Parr, 2009, Bhat et al., 2012]. Unfortunately, due to the nature of kernel learning, these algorithms can easily suffer from the curse of dimensionality, e.g. the required number of samples. Furthermore, kernel-based VFA algorithms can also have serious problems with over-fitting. As an alternative, *Neural Networks* (NN) have been employed to approximate value functions for decades [Lin, 1993, Bertsekas and Tsitsiklis, 1996]. Impressive successes of NNs in solving challenging problems in pattern recognition, computer vision, and speech recognition and game playing [LeCun et al., 2015, Yu and Deng, 2015, Mnih et al., 2015, Silver et al., 2017] have further triggered increasing efforts in applying NNs to VFA [van Hasselt et al., 2016]. More specifically, *NN-based Value Function Approximation* (NN-VFA) approaches have demonstrated their superior performance in many challenging domains, e.g. *Atari* games [Mnih et al., 2015] or the game *Go* [Silver et al., 2016, 2017]. Nevertheless, despite these advances, development of more efficient NN-VFA based algorithms is still of great demand for even more challenging applications. Currently, these impressive successes are only possible, if a plethora of training samples is available.

Aside from some early work in [Baird III, 1995], called *Residual Gradient* (RG) algorithms, omitting gradients of the TD-target has been a common practice, see e.g. [Riedmiller, 2005], and is referred to as *Semi-Gradient* (SG) algorithms [Sutton and Barto, 2020]. Reasons for choosing Semi-Gradients over Residual Gradients include inferior learning speed [Baird III, 1995], limitation with non-Markovian feature space [Sutton et al., 2008] and non-differentiable operators, e.g. the max-operator involved in Q-learning. In favour of Residual Gradients stand convergence guarantees and the applicability of “classic” gradient based optimization techniques.

In this work, we study the problem of minimising the *Mean Squared Bellman Error* (MSBE) with NN-VFA from the global analysis perspective, more specifically, in the framework of geometric optimisation [Absil et al., 2008]. We conduct a concise critical point analysis of the MSBE including its Hessian and also derive a proper approximation for it. We obtain insights in the learning process and can prevent the existence of saddle points or undesired local minima by requiring over-parametrisation of the NN-VFA and by ensuring certain properties of the optimisation objective. Furthermore, our analysis leads us naturally to an efficient and effective *Approximate Newton’s* (AN) algorithm. We investigate for a continuous state space setting whether or not ignoring the dependency of derivatives on the network parameters in the TD-target has a significant impact, especially in the context of second order optimisation. We outline how to overcome the convergence speed issues of Residual Gradients and show that gradients and higher order derivatives of the TD-target provide critical information about the optimisation problem. They are essential for implementing efficient optimisation algorithms and result in solutions with higher quality. Finally, we conduct several experiments to confirm the results of our critical point analysis numerically and also investigate the generalisation capabilities of NN-VFA empirically.

The rest of our paper is arranged as follows. In the next section we address the existing work regarding the construction and analysis of algorithms. In Section 3, we give a brief introduction to RL with VFA and provide the necessary notational conventions around NNs since a concise notation is required for our analysis in later sections. We conduct a critical point analysis of the MSBE when using NN-VFA in Section 4 and present our results separately for discrete and continuous state spaces in Sections 4.1 and 4.2, respectively. Section 5 is dedicated to our proposed Approximate Newton’s Residual Gradient algorithm and addresses details relevant for implementation. In Section 6 we evaluate performance and generalisation capabilities of the proposed method in several experiments. We end with a conclusion in Section 7.

2 Related Work

Recent attempts towards developing efficient NN-VFA methods follow the approach of extending the well-studied LVFA algorithms. These are a general family of gradient-based temporal difference algorithms, which have been proposed to optimise either the *Mean Squared Bellman Error* [Baird III, 1995, Baird III and Moore, 1999] or the *Mean Squared Projected Bellman Error* [Sutton et al., 2008, 2009]. The work in [Maei et al., 2009] adapts the results of developing the so-called *Gradient Temporal Difference* (GTD) algorithms to a non-linear smooth VFA manifold setting. The proposed approach requires projections onto the smooth manifold, which is practically infeasible because the geometry of VFA manifolds is in general not available. Similarly, the approach developed in [Silver, 2013] projects estimates of the value function directly onto the vector subspace spanned by the weight matrices of the NNs. Due to its intrinsic complexity, no further analysis or numerical development has been delivered besides the original work.

Such a difficulty in studying and developing NN-VFA methods is partially due to incomplete theoretical understanding of the optimisation of NNs. The main challenge of the underlying optimisation problem is the strong non-convexity. Although there are several efforts towards characterising the optimality of NN-training, e.g. [Kawaguchi, 2016, Nguyen and Hein, 2017, Haeffele and Vidal, 2017, Yun et al., 2018] a complete answer to the question is still quite demanding.

The work in [Shen, 2018b,a, Shen and Gottwald, 2019] addresses training of NNs using theory of differential topology and smooth optimisation. We aim at introducing those techniques to the RL domain.

Lately, there has been more interest in Residual Gradient algorithms. As described in [Baird III, 1995], Residual Gradient algorithms possess convergence guarantees since they use a complete gradient of a well-defined performance objective. Thus, they are eligible for a critical point analysis. Unfortunately, these guarantees are coupled to solving the *Double Sampling* issue, i.e., the requirement of having for any state several possible successors to capture stochastic transitions. In a recent submission [Saleh and Jiang, 2019] the authors explore the application of deterministic Residual Gradient algorithms to bypass the Double Sampling issue when using the *Optimal Bellman Operator*. Furthermore, they characterise empirically the impact of stepwise increased noise in environments and can motivate reviving Residual Gradient algorithms. We provide an investigation of Residual Gradient algorithms when using NNs for NL-VFA in deterministic problems, however, we address the Bellman Operator under some policy and work with Policy Iteration instead of aiming directly at the optimal value function.

We consider the work [Cai et al., 2019] also as strongly related to ours, as the authors pursue a similar idea, namely the importance of over-parametrisation. However, they address Semi-Gradient algorithms and thus work in a different setting. The authors show that the usage of NNs for NL-VFA with a redundant amount of adjustable parameters is mandatory for achieving good performance. They establish an implicit local linear linearisation and enable reliable convergence to a global optimum of the Mean Squared Projected Bellman Error. Similarly, in [Fu et al., 2019], authors arrive empirically at the conclusion that larger NL-VFA architectures result in smaller error and boost convergence. In [Liu et al., 2019] the role of over-parametrisation is classified as an important ingredient for a variant of *Proximal Policy Optimisation* [Schulman et al., 2017] to converge to an optimum. In our work we can confirm the role of over-parametrisation when using Residual Gradient algorithms and provide further insights from the global analysis perspective.

3 Notation

This section contains various definitions and provides a concise foundation for Section 4. First, we outline the Reinforcement Learning setting in general. Second, we introduce the usage of function approximation architectures and formulate the optimisation problem we want to investigate. Lastly, we define the function class and its components used for the NL-VFA method we are going to analyse.

3.1 Reinforcement Learning

Reinforcement Learning as a subset of Dynamic Programming represents methods to solve sequential decision making problems, e.g. they provide the automation for a robot or agent, which must perform actions in an environment based on its current state to increase a certain performance criterion. We model the decision making as a *Markov Decision Process* (MDP) by defining the tuple $(\mathcal{S}, \mathcal{A}, P, r, \gamma)$. We consider as state space \mathcal{S} both finite countable sets of K discrete elements $\mathcal{S} = \{1, 2, \dots, K\}$ as well as bounded subsets of finite dimensional Euclidean vector spaces $\mathcal{S} \subset \mathbb{R}^K$. Depending on the state space we denote by $K := |\mathcal{S}|$ either the cardinality of the finite set or by $K := \dim(\mathcal{S})$ the dimension of the vector space. The action space \mathcal{A} is always a finite set of discrete actions the agent can choose from. The conditional transition probabilities $P: \mathcal{S} \times \mathcal{A} \times \mathcal{S} \rightarrow [0, 1]$, which are either available directly in the form of analytic models or can be collected by using simulators and performing roll-outs, define for discrete spaces the probability $P(s'|s, a)$ for transiting from state s to s' when executing the action a . In continuous state spaces P takes the role of a probability density function which must be integrated over. A scalar *reward* function $r: \mathcal{S} \times \mathcal{A} \times \mathcal{S} \rightarrow [-M, M]$ with $M \in \mathbb{R}$ assigns an immediate and finite one-step-reward to the transition triplet s, a and s' . Finally, $\gamma \in (0, 1)$ represents a *discount factor* which is required to ensure convergence of the overall expected discounted reward.

The goal of an agent is to learn a *policy* π which maximises the expected discounted reward. It is sufficient to consider deterministic policies of the form $\pi: \mathcal{S} \rightarrow \mathcal{A}$, as the space of *history independent Markov policies* can be proven³ to contain an optimal policy. The expected discounted reward starting in some state $s \in \mathcal{S}$ and following the policy π afterwards is called *value function* and is defined as

$$V_\pi: \mathcal{S} \rightarrow \mathbb{R}, \quad s \mapsto \lim_{T \rightarrow \infty} \mathbb{E}_{s_1, s_2, \dots, s_T} \left[\sum_{t=0}^T \gamma^t r(s_t, \pi(s_t), s_{t+1}) \middle| s_0 = s \right]. \quad (1)$$

³e.g. chapter one and two in [Bertsekas, 2012], applies also to other statements in this section

It is well known that for a given policy π the value function V_π satisfies the *Bellman equation*, i.e., we can write for all states $s \in \mathcal{S}$

$$\begin{aligned} V_\pi(s) &= \mathbb{E}_{s'} \left[r(s, \pi(s), s') + \gamma \cdot V_\pi(s') \right] \\ &= \sum_{s'} P(s, \pi(s), s') \left(r(s, \pi(s), s') + \gamma V_\pi(s') \right), \end{aligned} \quad (2)$$

where s' is the successor state of s obtained by executing an action given by the policy π . The second equality in Equation (2) is only available if transition probabilities are known and exist due to discrete state and action spaces.

Treating V_π as a variable, the right hand side of Equation (2) is referred to as the *Bellman Operator* under the policy π and is denoted by $T_\pi: \mathcal{V} \rightarrow \mathcal{V}$, where \mathcal{V} is the space of all possible value functions. It can be shown that T_π is a contraction mapping with modulus γ and that the value function V_π under the policy π is its unique fix point. Hence, we can write

$$V_\pi(s) = (T_\pi V_\pi)(s) \quad \forall s \in \mathcal{S}. \quad (3)$$

Finally, we call for an arbitrary $V \in \mathcal{V}$ the difference of both sides in Equation (3) the *one-step Temporal Difference error*

$$\delta(s) := V(s) - (T_\pi V)(s) \quad \forall s \in \mathcal{S}. \quad (4)$$

The term *Temporal Difference* (TD) emphasizes the occurrence of the current state in $V(s)$ and the successor state s' in $(T_\pi V)(s)$. In this context one also calls the application of the Bellman operator *TD-target*. The TD-error is non-zero for all but the correct value function V_π . Thus, we can use δ to convert the fix point iteration into a root finding problem. By combining the squared TD-error for all states we obtain a performance objective that can be minimised. We will use this objective together with function approximation architectures to conduct our critical point analysis in a later section.

To ease the work with policies, it is possible to define similar to Equation (1) so called *Q-factors*

$$Q_\pi: \mathcal{S} \times \mathcal{A} \rightarrow \mathbb{R}, \quad s, a \mapsto \lim_{T \rightarrow \infty} \mathbb{E}_{s_1, s_2, \dots, s_T} \left[\sum_{t=0}^T \gamma^t r(s_t, \pi(s_t), s_{t+1}) \middle| s_0 = s, a_0 = a \right] \quad (5)$$

and the corresponding *Bellman equation in Q*

$$Q_\pi(s, a) = \mathbb{E}_{s'} \left[r(s, a, s') + \gamma \cdot Q_\pi(s', \pi(s')) \right] = (T_\pi Q_\pi)(s, a) \quad (6)$$

for all $s \in \mathcal{S}$ and $a \in \mathcal{A}$. While all algorithms work with *Q-factors* as they do for state-only value functions, it is now possible to define a *greedily induced policy* (GIP) compactly as

$$\pi': \mathcal{S} \rightarrow \mathcal{A}, \quad s \mapsto \operatorname{argmax}_{a \in \mathcal{A}} Q_\pi(s, a). \quad (7)$$

The improved GIP π' satisfies $\pi' \geq \pi$ in the sense that $Q_{\pi'}(s, a) \geq Q_\pi(s, a)$ for all states and actions with the equality being true for optimal policies.

3.2 Reinforcement Learning with Function Approximation

If a state space is finite but too large to be stored in memory, or even has to be treated as infinite due to its size, an exact representation of the value function $V_\pi(s)$ is practically impossible. This phenomenon is known as the *curse of dimensionality*. Also for continuous state spaces, where a proper iteration over all states is not available due to the lack of a natural discrete formulation, exact representations are out of reach. An accurate value function approximation is thus useful and necessary for representing the actual value function V_π of the current policy π in any computer system.

Let $F: \mathcal{S} \rightarrow \mathbb{R}$ be an arbitrary value function approximation and let us denote by \mathcal{V} the set of all possible approximations. If we further restrict the decision making problem to be *ergodic*, there exists a *steady state distribution* $\xi \in (0, 1)$ for each state⁴ which allows us to create a quality assessment for the approximation when combined with the aforementioned objective. The combination of a ξ -weighted norm and the TD-error of Equation (4) yields the *Mean Squared Bellman Error*

$$\text{MSBE}(F) = \frac{1}{2} \left\| F - (T_\pi F) \right\|_\xi^2, \quad (8)$$

which accepts a value function approximation $F \in \mathcal{V}$ and returns a scalar value. The factor $1/2$ is included for convenience. As the MSBE contains a norm over a function space, the realisation of the ξ -weighted norm comes in two

⁴for continuous spaces ξ is also a probability density function and must be used with integrals

different ways depending on the type of the state space. In discrete state spaces we can enumerate all states and write down directly

$$\text{MSBE}(F) = \frac{1}{2} \left\| F - (\text{T}_\pi F) \right\|_\xi^2 = \frac{1}{2} \sum_{s \in \mathcal{S}} \xi(s) \left(F(s) - (\text{T}_\pi F)(s) \right)^2. \quad (9)$$

Because the steady state distribution is a probability, we can interpret the right hand side as expectation and use samples to approximate it by the law of large numbers. We can write

$$\text{MSBE}(F) = \frac{1}{2} \mathbb{E}_{s \in \mathcal{S}} \left[\left(F(s) - (\text{T}_\pi F)(s) \right)^2 \right] \approx \frac{1}{2N} \sum_{i=1}^N \left(F(s_i) - (\text{T}_\pi F)(s_i) \right)^2, \quad (10)$$

where the samples s_i are drawn according to the environment. Changing from a ξ -weighted norm to e.g. a uniform weighting causes no harm. The steepest descent direction might change but the positions of critical points remain the same. In continuous spaces the ξ -norm is typically based on integrals

$$\text{MSBE}(F) = \frac{1}{2} \left\| F - (\text{T}_\pi F) \right\|_\xi^2 = \frac{1}{2} \int_{\mathcal{S}} \xi(s) \left(F(s) - (\text{T}_\pi F)(s) \right)^2 ds. \quad (11)$$

Here, ξ takes the roll of a normalised probability density function such that we can make use of Monte Carlo Integration. It allows us to write integrals as summations over many samples

$$\text{MSBE}(F) = \frac{1}{2} \int_{\mathcal{S}} \xi(s) \left(F(s) - (\text{T}_\pi F)(s) \right)^2 ds \approx \frac{1}{2N} \sum_{i=1}^N \left(F(s_i) - (\text{T}_\pi F)(s_i) \right)^2. \quad (12)$$

From Equations (10) and (12) it becomes clear that a realisation of an optimisation procedure for both types of state spaces results in the same instructions for a computer. However, as far as we are aware of, the the existence of the integral when working with continuous state spaces nor to the concise definition of a norm were part of the research focus in the past. The integrand $(F(s) - (\text{T}_\pi F)(s))$ in Equation (12) must be square integrable, i.e., be an element of L^2 . This is not a problem for the definition of V_π as the infinite discounted sum in Equation (1). Already necessary assumptions such as bounded rewards $|r(\cdot)| < M$ for some $M > 0$ and bounded state spaces guarantee square integrability. The system dynamics must be chosen to fit implicitly into these conditions. However, care must be taken for the selected function space \mathcal{V} . If using e.g. neural networks with arbitrary non-linearities as function class, square integrability might not be present. Furthermore, to define a norm, the integral should cover the whole Euclidean space, not only a bounded subset, to be inline with linearity requirements of any norm. However, this stands in conflict with the assumptions required for RL and also can affect in turn the square integrability of V_π . We postpone these theoretical concerns to the future.

The extension of the Mean Squared Bellman Error to Q-factors is in both settings straightforward. One has to add another sum or integral over all actions to definition of the MSBE and include the action as second input to F .

Reinforcement Learning with Function Approximation now manifests itself in the optimisation problem

$$F_\pi \in \underset{F \in \mathcal{V}}{\operatorname{argmin}} \text{MSBE}(F), \quad (13)$$

where F_π is the closest function to V_π in the approximation space \mathcal{V} . In general we have $F_\pi \neq V_\pi$ for at least some states $s \in \mathcal{S}$ and only aim to be close enough to V_π . By the choice of ξ as weighting for the norm, we also maintain for linear function approximation architectures the contraction properties of T_π when combining it with a linear projection onto that function space. The accuracy of the solution F_π as defined in Equation (13) is known to be bounded by

$$\|F_\pi - V_\pi\|_\xi \leq \frac{1 + \gamma}{1 - \gamma} \inf_{F \in \mathcal{V}} \|F - V_\pi\|_\xi. \quad (14)$$

Obviously, the challenge is to find a function space \mathcal{V} which we can optimise over and which still contains a good approximation for the desired function V_π . Thus, we investigate in Section 4 critical points of the MSBE and derive conditions, under which training results in finite exact approximations.

3.3 Multi Layer Perceptrons

To approximate value functions we deploy in this paper the classic feed forward fully connected neural network, a.k.a. *Multi-Layer Perceptron* (MLP). We summarize in the following the well-known definition of an MLP such that a concise notation for the remaining document exists for the reader with the goal to avoid any possible source of confusion.

Let us denote by L the number of layers in the MLP structure, and by n_l the number of processing units in the l -th layer with $l = 1, \dots, L$. By $l = 0$ we refer to the input layer with n_0 units. The value of n_0 depends on the state space and its type. For discrete spaces we have $n_0 = 1$ such that a single state can be processed as natural number directly by the network. In a continuous setting we use $n_0 = K$ units matching the K -dimensional state vectors. We always restrict the number of nodes in the output layer $l = L$ to $n_L = 1$.

Let $\sigma: \mathbb{R} \rightarrow \mathbb{R}$ be a unit activation function and denote by $\sigma': \mathbb{R} \rightarrow \mathbb{R}$ its first derivative with respect to the input. The unit activation function σ and its derivatives act element wise on non-scalar inputs. Depending on the concrete choice for σ the domain and image might have to be changed. Traditionally, the activation function σ is chosen to be non-constant, bounded, continuous and monotonically increasing (e.g. the *Sigmoid* function). More recent popular choices introduced unbounded functions like (*Leaky-*) *ReLU*, *SoftPlus* or the *Bent-Identity*⁵. In this work, we further restrict the choice for the activation function to *smooth*, *unbounded* and *strictly monotonically increasing* functions such as *SoftPlus*, *Bent-Identity* or also the *Identity* function itself as used in the last layer. The latter two are used in this work.

For the (l, k) -th unit in an MLP architecture, i.e., the k -th unit in the l -th layer, we define the corresponding *unit mapping* $\Lambda_{l,k}: \mathbb{R}^{n_{l-1}} \times \mathbb{R} \times \mathbb{R}^{n_{l-1}} \rightarrow \mathbb{R}$ as

$$\Lambda_{l,k}(w_{l,k}, b_{l,k}, \phi_{l-1}) := \sigma(w_{l,k}^\top \phi_{l-1} - b_{l,k}), \quad (15)$$

where $\phi_{l-1} \in \mathbb{R}^{n_{l-1}}$ denotes the output from layer $(l-1)$. The terms $w_{l,k} \in \mathbb{R}^{n_{l-1}}$ and $b_{l,k} \in \mathbb{R}$ are a weight vector and a scalar bias associated with the (l, k) -th unit, respectively. Next, we can define the l -th *layer mapping* by stacking all *unit mappings* of layer l as

$$\begin{aligned} \Lambda_l(W_l, b_l, \phi_{l-1}) &:= [\Lambda_{l,1}(w_{l,1}, b_{l,1}, \phi_{l-1}) \dots \Lambda_{l,n_l}(w_{l,n_l}, b_{l,n_l}, \phi_{l-1})]^\top \\ &= \sigma(W_l^\top \phi_{l-1} + b_l), \end{aligned} \quad (16)$$

with $W_l := [w_{l,1}, \dots, w_{l,n_l}] \in \mathbb{R}^{n_{l-1} \times n_l}$ being the l -th parameter matrix and $b_l := [b_{l,1}, \dots, b_{l,n_l}] \in \mathbb{R}^{n_{l-1}}$ the l -th bias vector. It is convenient to store the bias vector as an additional row of the matrix and extend the layer input with a constant value of 1. Thus, we can write Equation (16) equivalently as

$$\Lambda_l(W_l, \phi_{l-1}) := \sigma\left(W_l^\top \cdot \begin{bmatrix} \phi_{l-1} \\ 1 \end{bmatrix}\right) \quad (17)$$

by using a larger parameter matrix $W_l \in \mathbb{R}^{(n_{l-1}+1) \times n_l}$. Next, let us define the overall function represented by the MLP. First, denote by $\phi_0 \in \mathbb{R}^K$ the network input. Then, the output at the l -th layer is defined recursively as $\phi_l := \Lambda_l(W_l, \phi_{l-1})$. Note that the last layer in an MLP employs the identity map as activation function and is thus only a linear mapping. Finally, by denoting the set of all parameter matrices in the MLP by $\mathcal{W} := \mathbb{R}^{(n_0+1) \times n_1} \times \dots \times \mathbb{R}^{(n_{L-1}+1) \times 1}$ we can compose all layer-wise mappings to define for a set of parameters $\mathbf{W} \in \mathcal{W}$ the overall *network mapping* as

$$f: \mathcal{W} \times \mathbb{R}^{n_0} \rightarrow \mathbb{R}, \quad (\mathbf{W}, \phi_0) \mapsto \Lambda_L(W_L, \cdot) \circ \dots \circ \Lambda_1(W_1, \phi_0), \quad (18)$$

which contains in total N_{net} parameters with N_{net} being

$$N_{\text{net}} = \sum_{l=1}^L (n_{l-1} + 1) \cdot n_l. \quad (19)$$

With such a construction we can define the set of parametrised value functions belonging to a given MLP architecture by writing

$$\mathcal{F} := \{f(\mathbf{W}, \cdot): \mathbb{R}^{n_0} \rightarrow \mathbb{R} \mid \mathbf{W} \in \mathcal{W}\}. \quad (20)$$

With slight abuse of notation we refer by $\mathcal{F}(n_0, n_1, \dots, n_{L-1}, 1)$ to a concrete function class by specifying the architecture of the MLP, i.e., the number of processing units in each layer, as well as the input and out dimensions. Sometimes it is more convenient to describe an MLP by its depth d and the identical width w of all hidden layers. In this case we write $\mathcal{F}(n_0, w \times d, 1)$. The type of non-linearity is typically fixed and mentioned separately.

3.4 Optimisation Approaches

For solving the optimisation problem of Equation (13), i.e., obtaining the approximated value function with smallest MSBE, two fundamental approaches using steepest descent directions exist:

- *Direct Algorithms* [Baird III, 1995], alternatively called *Semi-Gradient* as proposed in [Sutton and Barto, 2020]

⁵also abbreviated as *Bent-Id*

- *Residual Gradient* algorithms [Baird III, 1995]

Both methods accept a parametrised function class such as MLPs with an initial set of parameters. Then, they move those parameters iteratively closer to an optimum by following repetitively a descent direction of the MSBE. Descent steps invoke derivatives of Equation (8) and the differential map of the MLP with respect to all parameters.

The difference of both approaches resides in the construction of derivatives. For Semi-Gradient algorithms, one ignores the dependence on the parameters through the value function inside the Bellman Operator. For Residual Gradient algorithms the *correct* gradient is calculated. The work [Zhang et al., 2020] provides a good summary and concise comparison about Semi-Gradient and Residual Gradient algorithms. Please refer to that paper and references therein for an overview over those algorithms and their advantages and disadvantages.

In the following, we proceed with the analysis of critical points of Equation (8) for discrete and continuous spaces. We only investigate Residual Gradient algorithms as there is no insight to be gained from a critical point analysis, when we use a direction for descending, which is not always pointing in the same half space as a gradient. Furthermore, we address to some extend the double sampling issue and outline possible solutions for slow convergence of Residual Gradients algorithm as described in [Zhang et al., 2020].

4 Theory

In this section we present our theoretical investigation of Residual Gradient algorithms by analysing the critical points of the Mean Squared Bellman Error. First, we investigate discrete state spaces and derive conditions under which learning a value function works reliably. Second, we extent our analysis to continuous spaces. We change to a sampling based approximation of the MSBE and adapt our conditions. We can characterise the importance of over-parametrisation, give design principles for MLPs and unveil a connection to other algorithms.

4.1 Critical Point Analysis for Discrete State Spaces

Consider MLPs of the form $\mathcal{F}(1, \dots, 1)$, i.e., fully connected feed forward networks with a one dimensional input and output and arbitrary depth or width. In discrete problems we have two choices to approach a critical point analysis. Either we want to have an approximation architecture that is exact for each of the K states or we are only interested in an architecture, which is exact for only $N \ll K$ sampled but unique states. While the second case simplifies the analysis and relaxes restrictions as shown later for continuous spaces, this also means that we have to address generalisation to states outside of the sampled ones. As the sampling case with discrete states would match almost completely our approach for continuous state spaces, we present here only the exact learning assumption. This means, we are interested in conditions for an MLP that would allow for a perfect solution to any state.

With discrete and finite spaces we can evaluate an MLP $f \in \mathcal{F}$ for every available state $s \in \mathcal{S}$ and collect the evaluations of f as vector in \mathbb{R}^K , where K is the number of states. As the most simple approach, we encode the discrete states as natural number for the single input unit and thus can treat $F(\mathbf{W}) := [f(\mathbf{W}, 1), \dots, f(\mathbf{W}, K)]^\top \in \mathbb{R}^K$ as the approximated value function for all states. Next, we can define the *Bellman Residual* for a policy π in matrix form as

$$\Delta_\pi(\mathbf{W}) = F(\mathbf{W}) - \mathbf{T}_\pi F(\mathbf{W}) = F(\mathbf{W}) - P_\pi \cdot (R + \gamma F(\mathbf{W})), \quad (21)$$

where we use a capital Δ instead of δ to emphasize that we consider all transitions in here instead of just a single one as in Equation (4). The term R contains the collection of all one-step-rewards suitable for the matrix form of the Bellman Operator and P_π is the transition probability matrix under policy π . By introducing a diagonal matrix $\Xi := \text{diag}(\xi_1, \dots, \xi_K)$ consisting of the steady state distributions ξ_i for all states, we can rewrite the norm in Equation (9) as the *Neural Mean Squared Bellman Error* (NMSBE) function

$$\mathcal{J}(\mathbf{W}) := \frac{1}{2} \Delta_\pi(\mathbf{W})^\top \Xi \Delta_\pi(\mathbf{W}). \quad (22)$$

It is important to notice that the NMBSE function is generally *non-convex* in \mathbf{W} , and, even worse, it is also *non-coercive* [Güler, 2010]: for $\mathbf{W} \rightarrow \infty$ we not necessarily have $\mathcal{J}(\mathbf{W}) \rightarrow \infty$. Thus, the existence and attainability of global minima of $\mathcal{J}(\mathbf{W})$ are not guaranteed in general. Nevertheless, when appropriate non-linear activation functions are employed in hidden layers, exact learning of finite samples can be achieved [Shah and Poon, 1999]. Analogously to the work in [Shen, 2018b], we have to assume that a specific MLP is able to approximate the value function V_π .

Assumption 1 (Existence of exact approximator). *Let $V_\pi : \mathcal{S} \rightarrow \mathbb{R}$ be the exact value function under policy π . For each state $s \in \mathcal{S}$ there exists at least one MLP architecture \mathcal{F} as defined in Equation (20) together with a set of parameters $\mathbf{W}^* \in \mathcal{W}$ such that the output of F and V_π coincide, i.e., we have*

$$f(\mathbf{W}^*, s) = V_\pi(s) \quad \forall s \in \mathcal{S}.$$

Additionally, we see that the error function, as it occurs as part of the NSMSE shown in Equation (22), follows Principle 1 in [Shen, 2018b]. For convenience, we repeat and translate this principle to our RL setting.

Principle 1 (Choice of error function). *The error function $E: \mathbb{R}^K \rightarrow \mathbb{R}$ is differentiable with respect to its only argument. If the gradient of E with respect to the argument vanishes at $V \in \mathbb{R}^K$, i.e., $\nabla E(V) = 0$, then V is a global minimum of E .*

As a first step, we identify the error function E in Equation (22) as

$$E: \mathbb{R}^K \rightarrow \mathbb{R}, \quad F \mapsto \frac{1}{2} (F - P_\pi(R + \gamma F))^\top \Xi (F - P_\pi(R + \gamma F)) \quad (23)$$

and see that it is differentiable in its only input. With such an E we could write the NMSBE also as $\mathcal{J}(\mathbf{W}) = E \circ F(\mathbf{W})$. As the next step we compute the gradient of E and obtain

$$\nabla_F E(F) = \left((F - P_\pi(R + \gamma F))^\top \Xi (I_K - \gamma P_\pi) \right)^\top, \quad (24)$$

where I_K is the $K \times K$ identity matrix. For the actual value function V_π the error function E vanishes by design and has a global minimum. Simultaneously, V_π causes the gradient to become zero as the Bellman Residual appears as a factor. Hence, E complies to Principle 1.

To conduct a critical point analysis of the NMSBE function we first have to compute the derivatives. By the linearity of the Bellman Operator T_π , we yield for the directional derivative of \mathcal{J} at the point $\mathbf{W} \in \mathcal{W}$ in direction $\mathbf{H} \in \mathcal{W}$

$$D\mathcal{J}(\mathbf{W})[\mathbf{H}] = \Delta_\pi(\mathbf{W})^\top \Xi (I_K - \gamma P_\pi) D F(\mathbf{W})[\mathbf{H}], \quad (25)$$

with $D F(\mathbf{W})[\mathbf{H}]$ being the differential map of the MLP. As the function $F(\mathbf{W})$ is simply a superposed function evaluated at each state, we just need to compute the directional derivative of the MLP evaluated at a specific state s , i.e. $D f(\mathbf{W}, s)[\mathbf{H}]$. Furthermore, the directional derivative of $f(\mathbf{W}, s)$ is a linear operator, hence the evaluation of the directional derivative of f for all states can be expressed as a matrix vector multiplication and results in

$$D F(\mathbf{W})[\mathbf{H}] = \underbrace{\left[\text{vec}(\nabla_{\mathbf{W}} f(\mathbf{W}, 1)), \dots, \text{vec}(\nabla_{\mathbf{W}} f(\mathbf{W}, K)) \right]^\top}_{=: G(\mathbf{W}) \in \mathbb{R}^{K \times N_{\text{net}}}} \text{vec}(\mathbf{H}), \quad (26)$$

where $\nabla_{\mathbf{W}} f(\mathbf{W}, s) \in \mathbb{R}^{N_{\text{net}} \times 1}$ is the gradient of f with respect to the parameters evaluated at \mathbf{W} for state s under the Euclidean norm. $\text{vec}(\cdot)$ transforms a matrix into a vector by stacking columns one after another. It acts on collections of matrices by concatenating the results of each individual vectorisation. The matrix $G(\mathbf{W})$ takes the role of the Jacobian for the evaluation of all states $F(\mathbf{W})$. Now, we can characterise critical points of the NMSBE function \mathcal{J} from Equation (22) by setting its gradient to zero, i.e., $\nabla_{\mathbf{W}} \mathcal{J}(\mathbf{W}) = 0$. By combining the results from Equations (25) and (26) together with *Riesz' Representation Theorem* we obtain the critical point condition of the NMSBE function as

$$\nabla_{\mathbf{W}} \mathcal{J}(\mathbf{W}) := \Delta_\pi(\mathbf{W})^\top \Xi (I_K - \gamma P_\pi) G(\mathbf{W})^\top \stackrel{!}{=} 0, \quad (27)$$

which is the counterpart⁶ to Equation (19) in [Shen, 2018b] for the Reinforcement Learning setting with discrete state spaces. Now we can derive the following proposition.

Proposition 1 (Suboptimal local minima free condition). *Let an MLP architecture \mathcal{F} satisfy Assumption 1 and the objective of Equation (22) be in accordance to Principle 1.*

If the rank of the matrix $G(\mathbf{W})$ as constructed in Equation (26) is equal to K for all $\mathbf{W} \in \mathcal{W}$ and $G(\mathbf{W})$ is non-zero, then any extremum $\mathbf{W}^ \in \mathcal{W}$ realises the true value function V_π , i.e., $f(\mathbf{W}^*, s) = V_\pi(s) \forall s \in \mathcal{S}$. Furthermore, the NMSBE function \mathcal{J} is free of suboptimal local minima.*

Proof. Because the underlying state transition matrix P_π of the MDP is required to be Markovian and ergodic, both terms Ξ and $(I_K - \gamma P_\pi)$ have full rank and are invertible. Consequently, the expression $\Xi (I_K - \gamma P_\pi) G(\mathbf{W})^\top$ also has rank K , if we claim that $G(\mathbf{W})$ has rank K and is non-zero. Hence, there is only the trivial solution left for the linear system in Equation (27), meaning that the Bellman Residual Δ_π must be exactly zero for all states. \square

The question under which conditions the matrix $G(\mathbf{W})$ has full column rank and is non-zero is the same as in [Shen, 2018b]. Being non-zero can still be ensured by choosing proper activation functions without zero derivatives for finite

⁶In this paper we used G in place of P to avoid confusion with the transition probability matrix

inputs. To see this we have to look at the structure of $G(\mathbf{W})$, which takes the form

$$G(\mathbf{W}) = \begin{bmatrix} \Psi_1^\top \left(I_{n_1} \otimes \phi_0^{(1)\top} \right) & \dots & \Psi_L^\top \left(I_{n_L} \otimes \phi_{L-1}^{(1)\top} \right) \\ \vdots & \ddots & \vdots \\ \Psi_1^\top \left(I_{n_1} \otimes \phi_0^{(N)\top} \right) & \dots & \Psi_L^\top \left(I_{n_L} \otimes \phi_{L-1}^{(N)\top} \right) \end{bmatrix}, \quad (28)$$

where the matrices $\Psi_l \in \mathbb{R}^{n_l \times n_L}$ and Kronecker products result from the layer wise definition of an MLP. The Ψ_l are products of diagonal matrices containing the derivative of σ and the parameter matrices of various layers, hence a proper choice for σ prevents $G(\mathbf{W})$ from becoming zero. A detailed construction is available in the appendix.

Maintaining the rank of $G(\mathbf{W})$ results in following all the design principles mentioned in [Shen, 2018b] to minimise the risk that rows of the differential map lie in a shared subspace. As in the multidimensional regression setting the overall block structure of $G(\mathbf{W})$ remains for RL applications. However, we have in the Reinforcement Learning setting the advantage that each block structure in $G(\mathbf{W})$ reduces to a single row compared to the regression setting, because the output layers are always scalar, i.e., $n_L = 1$. For the same amount of sampled inputs there are less possibilities to have linear dependent rows. While there are no theoretical guarantees, most matrices have full rank in practical applications where noise or sampling are present.

Unfortunately, the requirement of using over-parametrised MLPs

$$N_{\text{net}} \geq K \quad (29)$$

negates any useful insight. If we need as many adjustable parameters in an MLP as there are unique states, we could use a tabular representation in the first place and avoid dealing with non-linear function approximation. Please keep in mind that the strong condition in Equation (29) stems from the assumption of being exact for all states. If the NMSBE from Equation (22) is changed to be an approximation based on sampling, as done for continuous spaces in Section 4.2, we can reduce the number of MLP parameters from K down to $N \ll K$ samples. Thus, our theoretical investigation becomes applicable. At the same time generalisation becomes an issue, because the MLP is only accurate by design for finite many points in the state space. Investigating the predictive capabilities for the remaining states of a discrete space, which not necessarily has a proper definition for a metric, is out of the scope of this work.

With a sharp eye one can see that the differential map as shown in Equation (25) is a candidate for the *Gauss Newton* (GN) approximation as in the non-linear regression setting. Indeed, we have for the second directional derivative of \mathcal{J} at \mathbf{W} with two directions $\mathbf{H}_1, \mathbf{H}_2 \in \mathcal{W}$

$$\begin{aligned} D^2 \mathcal{J}(\mathbf{W})[\mathbf{H}_1, \mathbf{H}_2] &= \Delta_\pi(\mathbf{W})^\top \Xi(I_K - \gamma P_\pi) D^2 F(\mathbf{W})[\mathbf{H}_1, \mathbf{H}_2] \\ &\quad + (D F(\mathbf{W})[\mathbf{H}_1])^\top (I_K - \gamma P_\pi)^\top \Xi(I_K - \gamma P_\pi) D F(\mathbf{W})[\mathbf{H}_2], \end{aligned} \quad (30)$$

where we see that the first summand from the right hand side vanishes at any critical point $\mathbf{W}^* \in \mathcal{W}$. Thus, a good approximated evaluation of the Hessian of the NMSBE function at \mathbf{W}^* is given by

$$D^2 \mathcal{J}(\mathbf{W}^*)[\mathbf{H}_1, \mathbf{H}_2] = \text{vec}(\mathbf{H}_1)^\top \underbrace{G(\mathbf{W}^*)(I_K - \gamma P_\pi)^\top \Xi(I_K - \gamma P_\pi) G(\mathbf{W}^*)^\top}_{\mathbf{H}_W \mathcal{J}(\mathbf{W}^*) \in \mathbb{R}^{N_{\text{net}} \times N_{\text{net}}}} \text{vec}(\mathbf{H}_2). \quad (31)$$

This corresponds to the Gauss Newton approximation for non-linear least squares regression, i.e., defining the Hessian as the outer product of the Jacobian and its transpose. Our characterisation of critical points reveals this possibility for approximation as a side benefit. We also see from our derivation that one cannot naively use the outer product of the model's Jacobians $G(\mathbf{W}^*)$ as approximation, as this would ignore the additional structure coming from the Bellman Operator.

To ensure proper behaviour for a second order *Approximated Newton's* (AN) algorithm, we need to characterise the Hessian $\mathbf{H}_W \mathcal{J}(\mathbf{W}^*)$ of the NMSBE function at critical points as defined in Equation (31). The quadratic form leads to the following important result when combined with our design principles for MLPs.

Proposition 2 (Properties of the approximated Hessian). *The Hessian of the NMSBE function \mathcal{J} at any critical point \mathbf{W}^* is always positive semi-definite. Furthermore, its rank is bounded from above by*

$$\text{rank}(\mathbf{H}_W \mathcal{J}(\mathbf{W}^*)) \leq K,$$

if the MLP satisfies Equation (29).

Proof. Positive semi-definiteness of $\mathbf{H}_W \mathcal{J}(\mathbf{W}^*)$ follows from its symmetric definition. As before Ξ and $(I_K - \gamma P_\pi)$ have full rank. The rank of $G(\mathbf{W}^*)$ is at most K . For $\mathbf{H}_W \mathcal{J}(\mathbf{W}^*)$ being the product of these matrices we get the upper bound on its rank. \square

It is interesting to see that the rank condition from Equation (29) also allows the Hessian to become positive definite if the matrix $G(\mathbf{W})$ has full column rank. This has significant consequences for the optimisation problem. A positive definite Hessian at all critical points means that they are all true minima, thereby confirming Proposition 1. There are no saddle points or local maxima and thus a gradient based optimisation strategy cannot get stuck. Over-parametrisation of MLPs is thus not only important it is even necessary for Proposition 1 from the algorithmic perspective.

For the sake of completeness, we evaluate the proposed approximation for the Hessian in discrete state spaces empirically in Section 5.3. We demonstrate quadratic convergence of the Approximated Newton's algorithm indicating the validity of our approximation in the over-parametrisation setting. Repeated applications with reliable convergence to a global minimiser imply the absence of local minima or saddle points.

4.2 Critical Point Analysis for Continuous State Spaces

In high dimensional continuous state spaces, say $K > 6$, an exact representation of the value function based on a fine grained partitioning of \mathcal{S} is typically impossible. This is due to the *Curse of Dimensionality* and we are forced to work directly with the continuous space, which causes MLPs to be of the form $\mathcal{F}(K, \dots, 1)$ to accept K dimensional state vectors as input.

Since there cannot not exist a transition probability matrix in continuous spaces and its corresponding discrete steady state distribution Ξ , the NMSBE as shown in Equation (22) is not available here. We must work with a finite number of samples $N \in \mathbb{N}$ to approximate the loss as done in Equation (12). Another important limitation for Residual Gradient algorithms is the so called *Doubling Sampling Issue*. Due to the expectation inside the Bellman Operator for every single sample state $s_i \in \mathcal{S}$ many samples of possible successors $s'_i \in \mathcal{S}$ are necessary to approximate this expectation empirically. The *Double Sampling Issue* can be bypassed if an accurate model containing a description of stochastic transitions is available or if one has access to a simulator, where the state can be set freely to collect its successors. However, if one wishes to work in a pure model free manner or with rather limited and less powerful simulations, collecting successor samples becomes problematic. In a recent work [Saleh and Jiang, 2019] the authors also rediscovered the application of Residual Gradient algorithms in deterministic environments, motivated by the fact “that many empirical RL benchmarks are deterministic or only mildly stochastic [Brockman et al., 2016]” [Saleh and Jiang, 2019]. For our analysis, we follow the same strategy and restrict ourself to deterministic MDPs to analyse the algorithm in its purest form. As main consequence, we have to simplify the one step TD-error from Equation (4) for the i -th sample to

$$\delta(s_i, s'_i) := V(s_i) - r(s_i, \pi(s_i), s'_i) - \gamma V(s'_i) \quad \forall s_i \in \mathcal{S}, \quad (32)$$

where the successor state is produced according to the dynamical system under control, i.e., $s'_i = f(s_i, \pi(s_i))$. As before, we collect the evaluation of the MLP for all N sampled states s_i as vector in \mathbb{R}^N and denote it by $F(\mathbf{W}) := [f(\mathbf{W}, s_1), \dots, f(\mathbf{W}, s_N)]^\top \in \mathbb{R}^N$. The definition of $G(\mathbf{W}) \in \mathbb{R}^{N \times N_{\text{net}}}$ applies as in the discrete setting, detailed steps for its derivation are provided in the appendix. Next, we change the loss of Equation (12) accordingly and obtain the NMSBE for continuous state spaces as

$$\begin{aligned} \mathcal{J}(\mathbf{W}) &:= \frac{1}{2N} \sum_{i=1}^N \left(\underbrace{F(\mathbf{W}, s_i) - r(s_i, \pi(s_i), s'_i) - \gamma F(\mathbf{W}, s'_i)}_{\delta(s_i, s'_i)} \right)^2 \\ &= \frac{1}{2N} \begin{bmatrix} \delta(s_1, s'_1) & \dots & \delta(s_N, s'_N) \end{bmatrix} \cdot \begin{bmatrix} \delta(s_1, s'_1) \\ \vdots \\ \delta(s_N, s'_N) \end{bmatrix} = \frac{1}{2N} \Delta_\pi(\mathbf{W})^\top \Delta_\pi(\mathbf{W}), \end{aligned} \quad (33)$$

where $\Delta_\pi(\mathbf{W})$ now takes the form

$$\Delta_\pi(\mathbf{W}) = F(\mathbf{W}) - R - \gamma F'(\mathbf{W}) \quad (34)$$

when we denote by F' the evaluation of the MLP for all successor states. For this loss similar lines of thought apply as in the discrete setting. Yet we move at the same time closer to the learning setting and optimisation task from [Shen, 2018b]: We consider a finite set of sample states at which the corresponding value function is approximated exactly. Thus we adapt Definition 1 in [Shen, 2018b] for Residual Gradient algorithms.

Definition 1 (Exact Learning). *Let $V_\pi: \mathcal{S} \rightarrow \mathbb{R}$ be the value function under policy π . Given N sample states $s_i \in \mathcal{S}$ we call an MLP $f \in \mathcal{F}$, which satisfies*

$$f(\mathbf{W}, s_i) = V_\pi(s_i) \quad \forall i = 1, \dots, N$$

for some parameters $\mathbf{W} \in \mathcal{W}$, a finite exact approximator of V_π based on the N sample states.

As in the discrete setting, we can choose sufficiently rich MLP architectures \mathcal{F} and, thus, assume also in the continuous setting the existence of such an approximator.

Assumption 2 (Existence of finite exact approximator). *Let $V_\pi: \mathcal{S} \rightarrow \mathbb{R}$ be the value function of policy π . Given N unique samples $s_i \in \mathcal{S}$, there exists at least one MLP architecture \mathcal{F} as defined in Equation (20) together with a set of parameters $\mathbf{W}^* \in \mathcal{W}$ such that the MLP $f(\mathbf{W}^*, \cdot) \in \mathcal{F}$ is a finite exact approximator of V_π .*

We also see that the adapted NSMSE in Equation (33) still follows as error function Principle 1. We have

$$E: \mathbb{R}^N \rightarrow \mathbb{R}, \quad F \mapsto \frac{1}{2} (F - R - \gamma F')^\top (F - R - \gamma F') \quad (35)$$

which is differentiable and has the differential map

$$D E(F)[H] = (F - R - \gamma F')^\top (H - \gamma H'). \quad (36)$$

To define an actual gradient, a concrete choice for the function F is required to resolve the directions H and H' . However, we see already that the first term makes the map zero once we have a global optimum of the error itself. Hence, the adapted E still follows Principle 1 as it is required for Proposition 3 later on.

Our critical point analysis follows the same steps as in Section 4.1. First, we need the differential map of Equation (33). It takes the form

$$\begin{aligned} D \mathcal{J}(\mathbf{W})[\mathbf{H}] &= \frac{1}{N} \Delta_\pi(\mathbf{W})^\top \left(D F(\mathbf{W})[\mathbf{H}] - \gamma D F'(\mathbf{W})[\mathbf{H}] \right) \\ &= \frac{1}{N} \Delta_\pi(\mathbf{W})^\top \left(G(\mathbf{W}) - \gamma G'(\mathbf{W}) \right)^\top \text{vec}(\mathbf{H}), \end{aligned} \quad (37)$$

where G' is the Jacobian when using s'_i as input. Using this map critical points can be characterised by setting the gradient to zero

$$\nabla_{\mathbf{W}} \mathcal{J}(\mathbf{W}) := \frac{1}{N} \Delta_\pi(\mathbf{W})^\top \left(\underbrace{G(\mathbf{W}) - \gamma G'(\mathbf{W})}_{=: \tilde{G}(\mathbf{W}) \in \mathbb{R}^{N \times N_{\text{net}}}} \right)^\top \stackrel{!}{=} 0. \quad (38)$$

Apparently, the critical point condition for the continuous setting based on N unique samples in Equation (38) takes a similar form as that of the discrete setting in Equation (27). But since we no longer investigate the exact learning scenario we have to reformulate Proposition 1 and obtain a new version.

Proposition 3 (Suboptimal local minima free condition). *Let an MLP architecture $f \in \mathcal{F}$ satisfy Assumption 2 and the error function be in accordance to Principle 1.*

If the rank of the matrix $\tilde{G}(\mathbf{W})$ as defined in Equation (38) is equal to N for all $\mathbf{W} \in \mathcal{W}$ and $\tilde{G}(\mathbf{W})$ is non-zero, then any minimum $\mathbf{W}^ \in \mathcal{W}$ realises a finite exact approximator of V_π . Furthermore, the NMSBE function \mathcal{J} of Equation (33) is free of suboptimal local minima.*

Proof. Straightforward and mostly similar to Proposition 1. □

We now address the requirements for $\tilde{G}(\mathbf{W})$ since this matrix forms the backbone of Proposition 3. First, $\tilde{G}(\mathbf{W})$ has to be non-zero to define a proper equation system and enforce a trivial solution in terms of $\Delta_\pi(\mathbf{W})$ in Equation (38). For both differential maps $G(\mathbf{W})$ and $G'(\mathbf{W})$ the design principles apply individually. Hence it is unlikely in practice that for N unique sample states simultaneously both matrices vanish elementwise on their own. More troublesome is the distance between state s and its successor s' . If $\|s - s'\| \rightarrow 0$, which happens for example whenever s is getting close to a fix point of f , then the discount factor $\gamma \in (0, 1)$ prevents a perfect cancellation of $G(\mathbf{W})$ with $G'(\mathbf{W})$. Aside from those fix points in the state space it is again unlikely to observe in practice perfect cancellation of these two expressions.

As the second requirement the rank of $\tilde{G}(\mathbf{W})$ is important. Obviously, it is more difficult to make concise statements compared to discrete and exact learning setting. For the rank of the sum of two matrices the only known inequality is

$$\text{rank}(A + B) < \text{rank}(A) + \text{rank}(B),$$

which implies that we want still have to increase the rank of $G(\mathbf{W})$ and $G'(\mathbf{W})$ individually to push the upper bound for the rank of $\tilde{G}(\mathbf{W})$ high enough to allow for full rankness. This leads us to similar design choices for the MLP as in

the discrete setting. When taking a closer look at $\tilde{G}(\mathbf{W})$ itself, we find that the overall structure stays rather close to $G(\mathbf{W})$ from Equation (28). We have

$$\tilde{G}(\mathbf{W}) = \begin{bmatrix} \Psi_1^T \left(I_{n_1} \otimes \left(\phi_0^{(1)} - \gamma \phi_0'^{(1)} \right)^T \right) & \dots & \Psi_L^T \left(I_{n_L} \otimes \left(\phi_{L-1}^{(1)} - \gamma \phi_{L-1}'^{(1)} \right)^T \right) \\ \vdots & \ddots & \vdots \\ \Psi_1^T \left(I_{n_1} \otimes \left(\phi_0^{(N)} - \gamma \phi_0'^{(N)} \right)^T \right) & \dots & \Psi_L^T \left(I_{n_L} \otimes \left(\phi_{L-1}^{(N)} - \gamma \phi_{L-1}'^{(N)} \right)^T \right) \end{bmatrix}, \quad (39)$$

where the vectors $\phi_l \in \mathbb{R}^{n_l}$ result from the evaluation of all layers for state s and ϕ'_l from using s' . Again, we provide more detailed construction steps in the appendix. We see in Equation (39) that only the layer outputs ϕ get changed. Hence, the more complex $\tilde{G}(\mathbf{W})$ still complies to considerations of the discrete setting regarding linear dependent rows.

Of course these properties and requirements come without any guarantees, i.e., we expect that carefully constructed examples (yet almost pathological) exist where a drop of the rank of $\tilde{G}(\mathbf{W})$ happens. But in practice, where numerical errors and sampled quantities are present, this should not be much of a problem.

Various authors, e.g. the aforementioned work [Zhang et al., 2020] with the comparison of SG and RG formulation or [Baird III, 1995] directly, report a slow convergence of RG algorithms due to the similarity of $G(\mathbf{W})$ and $G'(\mathbf{W})$. We can identify two remedies here. The first is already visible in Equation (38) or Equation (39), where the contribution of the successor $G'(\mathbf{W})$ comes with the prefactor γ . If using multi-step lookahead the discount factor would come with higher powers, thus more efficiently taking away the cancelling effect of $G'(\mathbf{W})$ onto $G(\mathbf{W})$ if the successor stays after several steps still close to its original state. For large enough lookahead, γ^k would become small enough to allow for ignoring $G'(\mathbf{W})$ altogether, which also helps with the desired full rankness of $\tilde{G}(\mathbf{W})$. It is interesting to see that this multi-step lookahead in the objective resembles the construction of advantage estimators in *Proximal Policy Optimisation* [Schulman et al., 2017] or *Generalized Advantage Estimation* [Schulman et al., 2016]. Thus, Semi-Gradient issues such as the limited applicability of classic optimisation methods seem to be avoidable, because for long enough lookahead the omitted dependence of derivatives with respect to MLP parameters in the TD target vanishes naturally. The second remedy is related to the curvature of \mathcal{J} if s and s' are close by. The natural solution here is to employ second order gradient descent, again in the form of an Approximated Newton's algorithm: *Gauss Newton Residual Gradient Algorithm*. Other approaches to overcome curvature issues such as momentum based descent algorithms are too reliant on the dynamical runtime behaviour as well as on initialisation. They are prone to excessive hyper parameter tuning and frequent restarts. In the worst case, they complicate reproducibility, which is the reason why we decided to use second order optimisation.

As before, to see the possibility for the Gauss Newton approximation of the Hessian, we first write down the second order differential map of \mathcal{J} at point $\mathbf{W} \in \mathcal{W}$ for two directions $\mathbf{H}_1, \mathbf{H}_2 \in \mathcal{W}$

$$\begin{aligned} D^2 \mathcal{J}(\mathbf{W})[\mathbf{H}_1, \mathbf{H}_2] &= \frac{1}{N} \Delta_\pi(\mathbf{W})^T \left(D^2 F(\mathbf{W})[\mathbf{H}_1, \mathbf{H}_2] - \gamma \cdot D^2 F'(\mathbf{W})[\mathbf{H}_1, \mathbf{H}_2] \right) \\ &\quad + \frac{1}{N} \left(D \Delta_\pi(\mathbf{W})[\mathbf{H}_1] \right)^T \cdot \left(D F(\mathbf{W})[\mathbf{H}_2] - \gamma D F'(\mathbf{W})[\mathbf{H}_2] \right). \end{aligned} \quad (40)$$

Since the first summand contains the Bellman Residual as factor it vanishes at any critical point \mathbf{W}^* of \mathcal{J} due to the assumption of exact learning at sample states. This removes the contribution of second order derivatives of the MLP and allows us to simplify the Hessian to

$$D^2 \mathcal{J}(\mathbf{W}^*)[\mathbf{H}_1, \mathbf{H}_2] = \frac{1}{N} \text{vec}(\mathbf{H}_1)^T \underbrace{\left(G(\mathbf{W}^*) - \gamma G'(\mathbf{W}^*) \right) \cdot \left(G(\mathbf{W}^*) - \gamma G'(\mathbf{W}^*) \right)^T}_{\mathbf{H}_W \mathcal{J}(\mathbf{W}^*) \in \mathbb{R}^{N_{\text{net}} \times N_{\text{net}}}} \text{vec}(\mathbf{H}_2). \quad (41)$$

It becomes clear that proposition 2 applies almost unchanged.

Proposition 4 (Properties of the approximated Hessian). *The Hessian of the NMSBE function \mathcal{J} from Equation (33) is at any critical point \mathbf{W}^* always positive semi-definite. Furthermore, its rank is bounded from above by*

$$\text{rank}(\mathbf{H}_W \mathcal{J}(\mathbf{W}^*)) \leq N.$$

Proof. Positive semi-definiteness follows from the symmetric definition. The rank of the matrix $(G(\mathbf{W}^*) - \gamma G'(\mathbf{W}^*))$ is at most N . For $\mathbf{H}_W \mathcal{J}(\mathbf{W}^*)$ being the product of these we get the upper bound on its rank. \square

The question, whether $H_{\mathbf{W}}\mathcal{J}(\mathbf{W}^*)$ is positive definite or only semi-definite, is the same as in the discrete setting. We just have to use $\tilde{G}(\mathbf{W}^*)$ in place of $G(\mathbf{W}^*)$ alone and still arrive at

$$N_{\text{net}} \geq N \quad (42)$$

to allow the rank to become full. We want to emphasize that this requirement for the Hessian is far less restricting than in the discrete setting with exact learning. Also computational concerns regarding a second order optimisation method are no longer that severe with nowadays hardware capabilities. MLPs can become large enough for RL applications while still allowing for working with Hessians in a reasonable time. We further address practical concerns in Section 5 and as part of the experiments. Lastly, the question how many sample states are required, i.e., how to select the size of N for a certain MDP, enters the realm of sampling complexity and is out of the scope of this work.

5 A Gauss Newton Residual Gradient Algorithm

In this section we provide details regarding our concrete algorithm, which are based on the results from the theory section. The focus lies on aspects that are relevant on their own, i.e., decoupled from any experiment, but fit no longer into the previous section, as they are only due to the implementation in a computer system. We give pseudo code as it is used in the experiments and demonstrate numerically the correctness of our approximated Hessian using the discrete exact learning setting.

5.1 Second Order Algorithms

Second order gradient descent algorithms seek for roots in the gradient vector field. Thus, they are also attracted by local maxima or saddle points. However, these types of extrema, if they exists as we elaborate after Propositions 2 and 4, are numerically unstable. This means that as long as we do not hit exactly those points the optimisation will follow a descent direction towards a minimum.

A typical concern regarding second order algorithms is the computational effort involved in models with many parameters. Typical architectures of MLPs used in RL applications contain around two hidden layers with approximately 50 units in each layer. For such MLPs N_{net} falls in the range of ~ 2000 parameters, for which second order optimisation is manageable with reasonable time and storage as we demonstrate with our experiments.

The Approximated Newton's step $\eta \in \mathcal{W}$ is the solution of a regularised linear system using the gradient from Equation (37) and the Hessian from Equation (41). We must solve

$$(H_{\mathbf{W}}\mathcal{J}(\mathbf{W}) + c \cdot I_{N_{\text{net}}}) \cdot \eta = \nabla_{\mathbf{W}}\mathcal{J}(\mathbf{W}), \quad (43)$$

where $c = 10^{-5}$ controls the strength of regularisation. We use this value for all experiments if not otherwise stated. The regularisation is important because the approximated Hessian is only valid in a restricted neighbourhood around critical points. Outside of critical points, the regularisation ensures that the gradient is part of the Newton's direction η . This disturbance also helps with avoiding saddle points, as the descent direction is not completely coinciding with a correct Newton's direction if one hits a critical point exactly.

We did not make use automatic differentiation frameworks due to the following reasons. First, they are *not* able to introduce approximations to symbolic expressions on their own. As we already have the required differential maps available due to our theoretical investigation, we could realise the optimisation procedure by hand without too much overhead. Second, to best of our knowledge, the operations involved in the Hessian are not suited for general purpose graphics processing units, hence the performance gain of automatic differentiation frameworks is minimal. Third, as we have to solve a linear equation systems we cannot avoid to use other libraries as well, which would add additional overhead in the data transfer. In conclusion, by implementing the algorithm manually we achieved the full control over all the components and also could make use of sophisticated parallelisation. Of course, recent developments and contributions to automatic differentiation frameworks can render these considerations obsolete.

5.2 Pseudocode

For our experiments we need two kinds of algorithms. The first is *Policy Evaluation* as shown in Algorithm 1. It makes uses of a Gauss Newton Residual Gradient algorithm to approximate V_{π} with a given MLP. The required inputs are initial parameters for the MLP as well as a policy to evaluate. As output one obtains the optimal parameters.

The second algorithm is just full *Policy Iteration*, which makes use of the first algorithm and extends it with a *Policy Improvement* step. After every sweep consisting of evaluation and improvement a better performing policy should be available. It is depicted in Algorithm 2.

Algorithm 1 Policy Evaluation with Gauss Newton Residual Gradient Algorithm

```

1: Hyper parameters:  $\gamma \in (0, 1)$ ,  $\alpha > 0$ ,  $c = 10^{-5}$ ,  $\epsilon \leq 10^{-5}$ ,  $N \sim N_{net}$ 
2: Input: MLP  $f \in \mathcal{F}(n_0, \dots, 1)$  with weights  $\mathbf{W} \in \mathcal{W}$ , policy  $\pi$ ,
3: Output:  $\mathbf{W}$  such that  $f(\mathbf{W}, s_i) \approx V_\pi(s_i) \quad \forall i = 1, \dots, N$ 

4: Sample  $N$  unique states  $s_i \in \mathcal{S}$  and construct transition tuples  $s_i, r_i, s'_i$ 
5: Evaluate  $F(\mathbf{W}) := [f(\mathbf{W}, s_1), \dots, f(\mathbf{W}, s_N)]^\top \in \mathbb{R}^N$  and its differential map  $G(\mathbf{W})$ .
6: Similarly, evaluate  $F'$  and  $G'$ .

7: do

8:   NMSBE:  $\mathcal{J}(\mathbf{W}) = \frac{1}{2N} \Delta_\pi(\mathbf{W})^\top \Delta_\pi(\mathbf{W})$ 
9:   Gradient:  $\nabla_{\mathbf{W}} \mathcal{J}(\mathbf{W}) = \frac{1}{N} \Delta_\pi(\mathbf{W})^\top (G(\mathbf{W}) - \gamma G'(\mathbf{W}))^\top$ 
10:  Hessian:  $\mathsf{H}_{\mathbf{W}} \mathcal{J}(\mathbf{W}) = \frac{1}{N} (G(\mathbf{W}) - \gamma G'(\mathbf{W})) \cdot (G(\mathbf{W}) - \gamma G'(\mathbf{W}))^\top$ 
11:  Solve for  $\eta$ :  $(\mathsf{H}_{\mathbf{W}} \mathcal{J}(\mathbf{W}) + c \cdot I_{N_{net}}) \cdot \eta = \nabla_{\mathbf{W}} \mathcal{J}(\mathbf{W})$  (e.g. with Householder QR-Decomposition)
12:  Descent step:  $\mathbf{W} \leftarrow \mathbf{W} - \alpha \eta$ 

13: while  $\mathcal{J}(\mathbf{W}) > \epsilon$ 

```

A common practice in Policy Iteration is to reuse the most recent evaluation outcome for the next iteration. In [Sigaud and Stulp, 2019] this practice is called *persistent* while running the evaluation from scratch in every sweep is referred to as *transient*. We employ this naming convention here as well.

Algorithm 2 Policy Iteration

```

1: Hyper parameters:  $\gamma \in (0, 1)$ ,  $\alpha > 0$ ,  $c = 10^{-5}$ ,  $\epsilon \leq 10^{-5}$ ,  $N \sim N_{net}$ ,  $sweeps > 0$ 
2: Input: MLP  $f \in \mathcal{F}(n_0, \dots, 1)$  with weights  $\mathbf{W} \in \mathcal{W}$ ,
3: Output: policy  $\pi$ 

4:  $\mathbf{W} \leftarrow UniformInitialisation(-1, 1)$ 
5:  $\pi(s) \leftarrow GIP(f, \mathbf{W}, s)$  for all  $s \in \mathcal{S}$ 

6: for sweep in sweeps do

7:   if not persistent then
8:      $\mathbf{W} \leftarrow UniformInitialisation(-1, 1)$ 
9:   end if

10:   $\mathbf{W} \leftarrow PolicyEvaluation(f, \mathbf{W}, \pi)$ 
11:   $\pi'(s) \leftarrow GIP(f_\pi, \mathbf{W}, s)$  for all  $s \in \mathcal{S}$ 
12:  Evaluate  $\pi'$  using several roll-outs
13:   $\pi \leftarrow \pi'$ 

14: end for

```

5.3 Demonstration of Quadratic Convergence using a Discrete State Space

To evaluate empirically our derived theoretical results in the discrete state space setting together with the assumption of exact learning we demonstrate quadratic convergence on Baird's *Seven State Star Problem* [Baird III, 1995]. Only if all components work as intended quadratic convergence of a second order gradient descent algorithm can be visible. As we require a problem where all states occur infinite many times for the NMSBE to be well-defined, we extend the *Star Problem* with transitions from the single node to all others. Please refer to Figure 1 to see all transitions and their probabilities. A policy for evaluation is defined implicitly by setting the transition probabilities to fixed values. The reward is present in *state 1* and takes the value 1. As discount factor we use $\gamma = 0.99$.

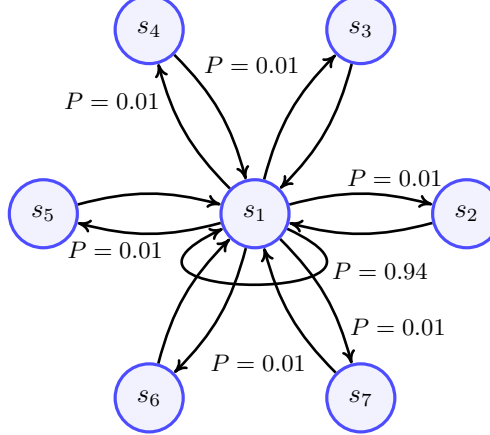


Figure 1: Adapted version of Baird’s *Seven State Star Problem* [Baird III, 1995]. We have added transitions with low probabilities from the centre back to the six outer states to obtain an infinite horizon problem such that the the NMSBE is well-defined.

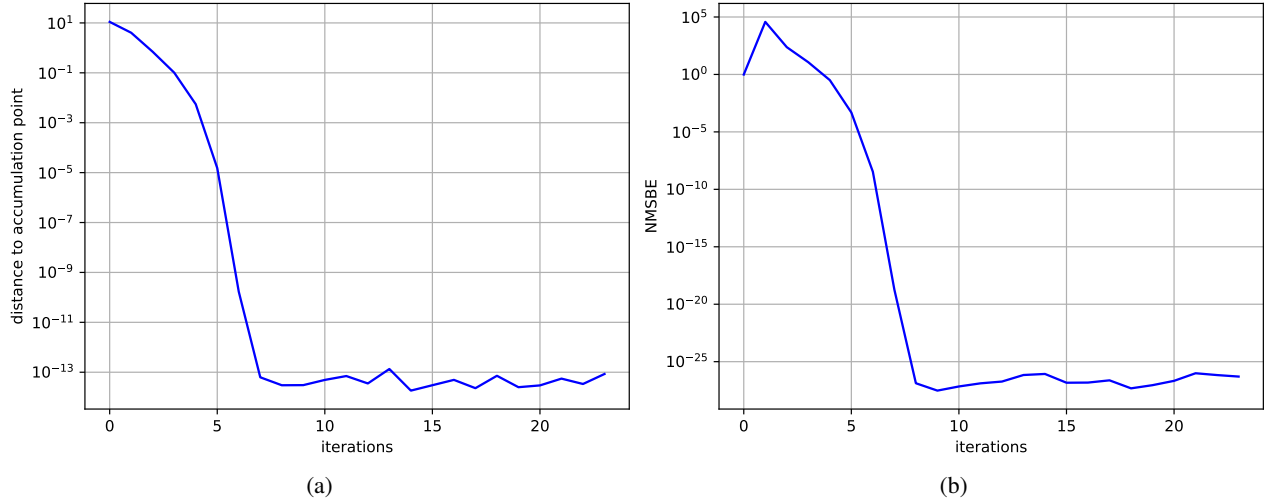


Figure 2: Local quadratic convergence on adapted version of Baird’s *Seven State Star Problem*. **a)**: Distance of iterates $\mathbf{W}^{(k)}$ to the accumulation point \mathbf{W}^* . **b)**: The NMSBE corresponding to each iterate.

We deploy an MLP architecture $\mathcal{F}(2, 7, 1)$ consisting of $N_{net} = 29$ parameters with step size $\alpha = 1$ and use *Bent-Id* as activation function in hidden layers. Every state receives a unique two-dimensional random feature to embed the discrete states in a vector space for the input layer. Features are drawn from a normal distribution with zero mean and unit covariance.

In Figure 2 we visualise convergence with the distance of the accumulation point \mathbf{W}^* to all iterates $\mathbf{W}^{(k)}$ as well as by the corresponding NMSBE. We use the last iterate as \mathbf{W}^* and measure the distance by extending the Frobenius norm of matrices to collections of matrices as $\|\mathbf{W}^{(k)} - \mathbf{W}^*\|_F^2 := \sum_{l=1}^L \|W_l^{(k)} - W_l^*\|_F^2$.

It is clear from Figure 2a that the AN algorithm converges locally quadratically fast to a minimiser. From Figure 2b we conclude that the MLP is close to the ground truth value function as the NMBSE becomes negligibly small. Both graphs together imply that the approximation of the Hessian is valid close to \mathbf{W}^* and additionally that its rank is full. Due to the over-parametrisation convergence to suboptimal local minima does not happen.

6 Numerical Experiments in Continuous State Spaces

In this section we describe our experiments. First, we outline the experimental setup. Second, we investigate the convergence behaviour in continuous state spaces. We compare Residual Gradients with Semi-Gradients and investigate

the influence of second order optimisation. Next, we explore the generalisation capabilities of an MLP when trained with a Gauss Newton Residual Gradient algorithm by evaluating the NMSBE on unseen states outside of the training set. Finally, we address the application of a second order Residual Gradient algorithm in full Policy Iteration and test it in a continuous control problem.

6.1 Experimental Setup

We investigate the application of a Gauss Newton Residual Gradient algorithm for Policy Evaluation in finite dimensional and bounded Euclidean state spaces. We provide empirical results for the performance of the Approximated Newton's algorithm by minimising the objective of Equation (33) in several different scenarios:

1. **Convergence of Policy Evaluation** by evaluating the value function of a fixed policy
2. **Generalisation Capabilities** by characterising the influence of different MLP architectures on the generalisation performance
3. **Full Policy Iteration** by combining Policy Evaluation and Q-factors to improve iteratively an initial policy

Investigating the performance of the algorithm with generalisability in mind is both interesting and important due to the still-unexplainable generalisability of neural networks [Lawrence et al., 1997, Zhang et al., 2017, Neyshabur et al., 2017]. Testing in a full *Policy Iteration* setting is important for the general applicability of a Gauss Newton Residual Gradient algorithm.

In our Policy Evaluation experiments, except for generalisation, we compare the cases of whether or not considering derivatives of the TD-target. This means we compare Semi-Gradient and Residual Gradient formulations for both first and second order optimisation methods.

For the experiments, we use the *Mountain Car* [Moore, 1990] and the *Cart Pole* control problems [Barto et al., 1983] as environments. These two are classic deterministic Reinforcement Learning benchmarks with a typical continuous state space and a manageable complexity that allows for an extensive investigation and visualisation. More specifically, we employ the *MountainCar-v0* of the *OpenAI Gym* package [Brockman et al., 2016], and include an important change to the reward function: We replace the built-in constant reward function, which assigns independently of the state, action and successor state to *any* transition the punishment -1 , with a function that rewards being in a goal region by not giving punishments in that area. We define the goal region as $x > 0.5$, where x denotes the position of the car. Once the car enters the goal region we teleport it back to a starting state. These two adjustments allows us to use the environment in a non-episodic fashion and, thereby, establish the required formulation of the MDP to work with uniformly sampled state transitions. Similarly, the *CartPole-v1* world of *OpenAI Gym* receives a new non-constant reward. Instead of rewarding every step with $+1$, including those states which are considered to be a failure because the pole fell over or the cart left the allowed range, we only punish with -1 reward the transition into those failure states. Otherwise, the reward is zero. Finally, by adding connections from terminal to start states, we convert the episodic formulation of the balancing task and restore also here an infinite horizon MDP. We set the discount factor for all environments to $\gamma = 0.99$ if not otherwise stated.

6.2 Empirical Convergence Analysis

Setting We first make use of the *Mountain Car* problem, which has a continuous state space and discrete actions, and investigate the performance when evaluating a predefined policy. The complexity and dimensionality of the problem is manageable, which enables us to estimate the ground truth value function with Monte Carlo methods based on a fine grained two dimensional grid. Thus, we can evaluate accurately the performance of tested algorithms against the ground truth. The policy, whose value function is being evaluated, is fixed to accelerate the car in the direction of the current velocity.

We investigate the performance of the algorithm under the influence of three variants: *ignoring TD targets in derivatives*, *using Hessian based optimisation* and *varying learning rates*. We use four different learning rates $\alpha \in \{10^0, 10^{-1}, 10^{-2}, 10^{-3}\}$ and study all sixteen combinations.

For all tests, we adopt the batch learning scenario. Specifically, we use as the training set 100 transition tuples (s, r, s') collected in prior with the fixed policy. States s are sampled uniformly from \mathcal{S} . Executing the action provided by the policy in each state yields its successor s' and the one-step-reward r for that transition. We fix the transition tuples throughout all convergence experiments to provide a fair comparison between individual runs.

As function space for approximated value functions, we employ the MLP $\mathcal{F}(2, 10, 10, 1)$ with *Bent-Id* activation functions. This architecture has $N_{net} = 151$ free parameters, i.e., more parameters than the number of samples, and

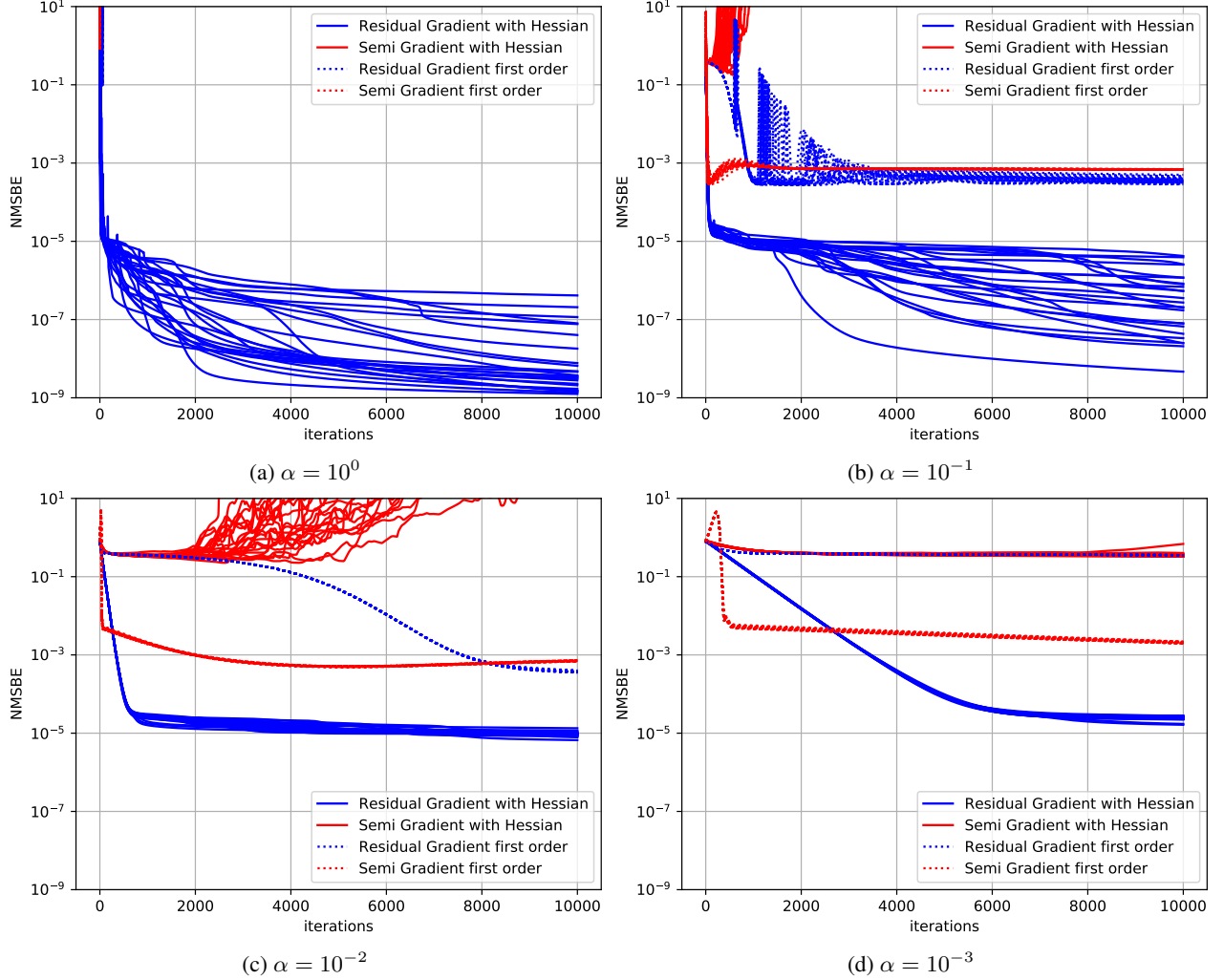


Figure 3: The NMSBE as defined in Equation (33) plotted over time for all tested optimisation approaches. Figure a) to d) represent considered learning rates $\alpha \in \{10^0, 10^{-1}, 10^{-2}, 10^{-3}\}$. A Residual Gradient formulation combined with Hessian based optimisation outperforms Semi-Gradient algorithms for all learning rates and stays convergent, even for large values of α . First-order only Residual Gradient algorithms demonstrate the reported slow convergence.

thus complies to our theoretical findings. Furthermore, MLPs in this experiment are all initialised with the same weight matrices to further improve the comparability. For the initialisation we use a uniform distribution in the interval $[-1, 1]$.

Although there is no noise or randomness in the environment part involved and we do not make use of exploration mechanisms, the outcomes can still vary. We use an asynchronous multithreaded implementation such that numerical errors can either accumulate or cancel out over time based on the order of execution. Hence, all experiments are repeated 25 times. Our results of the optimisation processes are shown in Figure 3.

Results We observe that a Semi-Gradient algorithm always diverges for extremely large step sizes as shown in Figure 3a with $\alpha = 1$. For the smaller step sizes $\alpha \in \{10^{-1}, 10^{-2}, 10^{-3}\}$ as shown in Figures 3b, 3c and 3d a Semi-Gradient algorithm can converge if using first order optimisation. Extending it to second order gradient descent causes it to diverge sooner or later for all step sizes. For small enough learning rates, e.g. $\alpha = 10^{-3}$, second order Semi-Gradient additionally achieves only the same final NMSBE as first-order Residual Gradient methods, indicating that the computation for the approximated Semi-Hessian is obsolete. However, we want to point out that the resulting solution of Policy Evaluation is not good compared to other possible outcomes.

Figures 3b and 3c show that first order gradient descent algorithms with and without ignoring the dependency of the gradient on the TD target perform consistently and achieve almost identical final errors. Looking at the descent

behaviour, we can confirm the slow convergence issue of a Residual Gradient formulation. From Figure 3d it becomes clear that first order Semi-Gradient descent combined with carefully selected learning rates $\alpha \in \{10^{-2}, 10^{-3}\}$ can achieve an equal or even lower final error, further explaining its popularity over Residual Gradients.

In contrast stands the Gauss Newton Residual Gradient algorithm, i.e., a Gauss Newton algorithm combined with *complete* derivatives of the NMSBE. This algorithm works well with all learning rates, in particular this algorithm works with large learning rates as it can be seen in Figures 3a and 3b. Furthermore, the final value for the NMSBE is orders of magnitude smaller than that of other approaches. Finally, the algorithm also performs consistently for extremely large learning rates $\alpha = 1$. Despite strong initial numerical problems all repetitions arrive at a sufficiently small NMSBE over time. In other words, building the derivatives of the TD target w.r.t. to the parameters and using (approximate) second order information of the NMSBE function are important ingredients for designing and implementing efficient NN-VFA algorithms. Modifying the descent direction based on the curvature is crucial to achieve good performance. This insight matches also the empirical evidence that when combining Semi-Gradient algorithms with annealing schemes for learning rates even better performance can be obtained [Gronauer and Gottwald, 2021].

Computational concerns A severe burden of Newton-like algorithms is the computational complexity involved in the Hessian, especially since the Gauss Newton approximation involves a full sized and dense Hessian. In this experiment, first order only methods require roughly 8.4 and 7.6 seconds on average for 10^4 iterations of Semi- and Residual Gradients, respectively. Calculating the Hessian and Newton’s direction⁷ increases the run time to 22.4 and 48.5 seconds, respectively. These run times are not supposed to be accurate measurements but should just reveal the overall trend. The numbers imply that within 10^4 steps of a first order Residual Gradient method only around 1500 iterations of a Gauss Newton Residual Gradient algorithm can be performed on our computers. However, the performance gain in terms of convergence speed and overall lower error, as seen in Figure 3b or Figure 3c, still justifies the additional computational effort. A second order algorithm is overall *faster* than first order only methods, because far less iterations are required to reach an already significantly smaller error. The performance could be further enhanced if we would make use of concepts such as the Levenberg-Marquardt heuristic or put additional effort in hyper parameter tuning.

6.3 Generalisation Capabilities of MLPs

As mentioned earlier in the theoretical analysis of discrete and exact learning, working with finite exact approximators based on N samples from a continuous state space makes generalisation an important topic. Since the approximated value function can only be trained to fit a finite set of samples, the generalisation capabilities of an MLP for states in between the collected training samples are essential to RL and are worth further investigation. Thus, we evaluate an approximated value function, which we obtain by optimising the NMBSE with the Gauss Newton Residual Gradient algorithm, with states that were not part of the training data.

6.3.1 Single Architecture

Setting We start with a single architecture and vary the amount of training samples. More specifically, we consider again the MLP $\mathcal{F}(2, 10, 10, 1)$ with learning rate $\alpha = 10^{-2}$ and *Bend-Id* activation function. For the initialisation we use a uniform distribution in the interval $[-1, 1]$. For this experiment, we vary the number of training samples N non-uniformly between 25 and 2000 and compute the NMSBE for a separated test set comprised of $25 \cdot 10^4$ states arranged on a grid. Again, we repeat for each N the training of MLPs 25 times and visualise the NMSBE as box-plots in Figure 4a for the training data and in Figure 4b for the held-out test set.

Results It is clear that at $N = 2000$ the training process is always successful with almost ignorable variance. While decreasing the number of randomly placed training samples down to $N = 300$, the mean error becomes slightly larger with more pronounced variances. Furthermore, only poor results are observed at $N = 25$. Here, the MLP is able to fit the training data exactly, however, the test error indicates that this is no longer a valid solution.

We observe for the test error that the variance when using $N = 150$ samples is smaller than that for its direct neighbours. Similarly, there is a sharp reduction in the variance for training errors starting at $N = 125$. Since these numbers of samples is almost identical or at least close to the number of parameters in the network ($N_{\text{net}} = 151$) this could be a numerical confirmation of the theoretical condition as derived earlier, however, we admit that an empirical verification is rather involved. In particular, we require N unique samples in the training set, but there is no practical way to determine, whether those N collected samples are “sufficiently unique”.

⁷using *Eigen*’s Householder QR-decomposition when linked against *OpenBlas* and *OpenLapack*

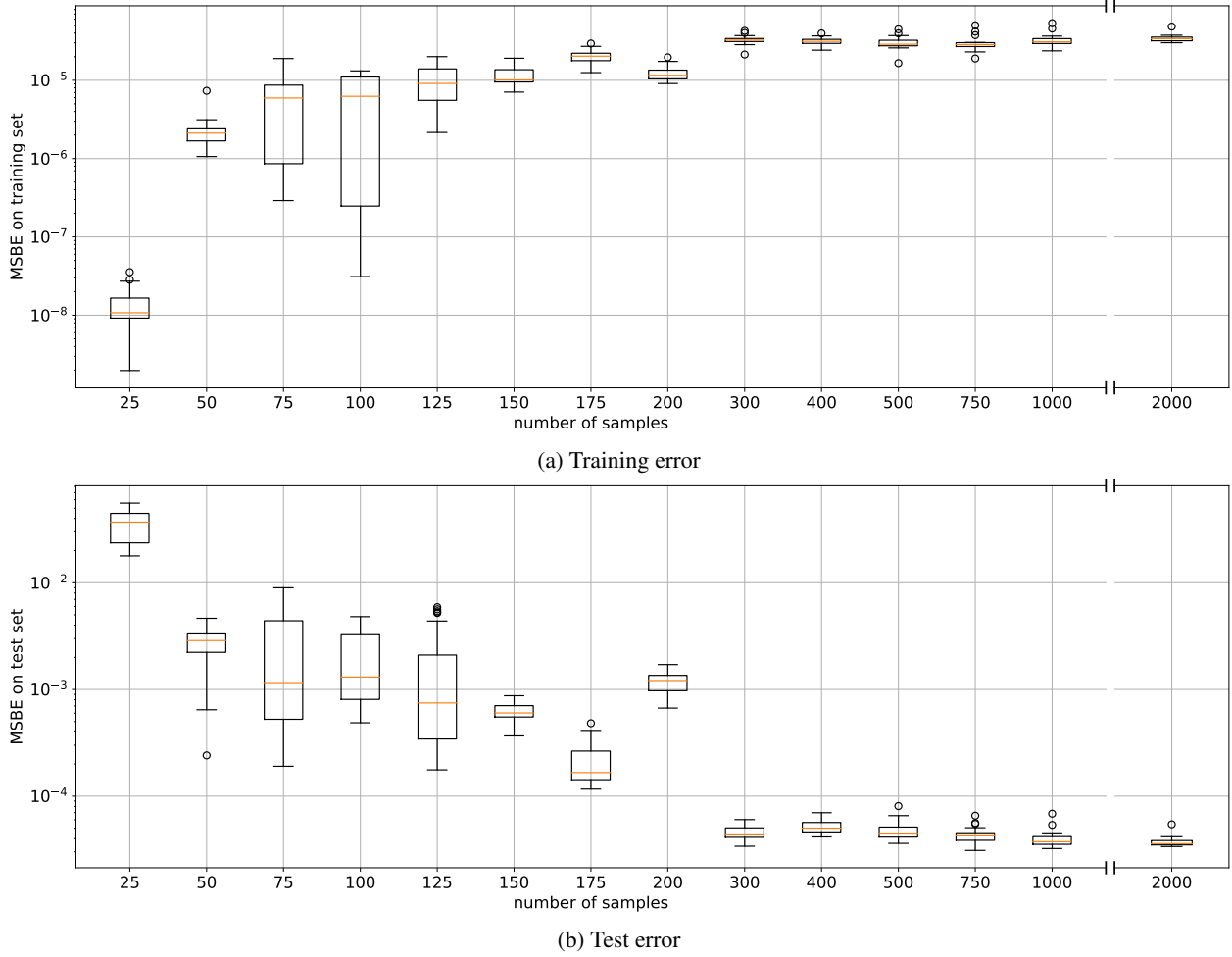


Figure 4: The final NMSBE of the MLP $\mathcal{F}(2, 10, 10, 1)$ for different amount N of training samples. **Top:** NMBSE using the training samples. **Bottom:** NMSBE for the test set.

When evaluating the approximated value function with smallest test error for $N = 25$ samples visually, i.e., see Figure 5b, one can spot a plateau located at around -100 expected discounted reward. This is exactly the solution to Bellman's equation or to the loss as defined in Equation (33) if every transition would yield -1 reward. This indicates that those scarce samples do not allow the reward information to flow and hence we have solved implicitly a different MDP. By comparing the ground truth value function as shown in Figure 5a, which we obtain by running rollouts from every grid state in the test set, to other value functions learned with different sample sizes as shown in Figures 5c to 5f, we see that training with even only 50 samples starts to fit the shape of the ground truth value function in the correct range. Hence, this experiment suggests that for problems with a continuous state space, NN-VFA methods can still perform well with a relatively small number of sampled interactions.

6.3.2 Various Architectures

Setting It is widely believed that the architecture of an MLP has an important influence on its generalisation performance, but the exact impact is still unclear. Therefore, we train several MLPs of different architecture and a varying number of samples in the same scenario as above. Please refer to the axis labels in Figure 6 for concrete choices of architectures and the values of N . Due to the huge amount of computation involved in deeper networks with large sample sizes we reduce the number of repetitions from 25 to 10. We provide the mean test and training error as contour plots in Figure 6 in logarithmic scale ($Z = \log_{10}(E)$ where E is the actual error and Z its plotted value). This additional processing step is required to reveal the detailed structure of the surface.

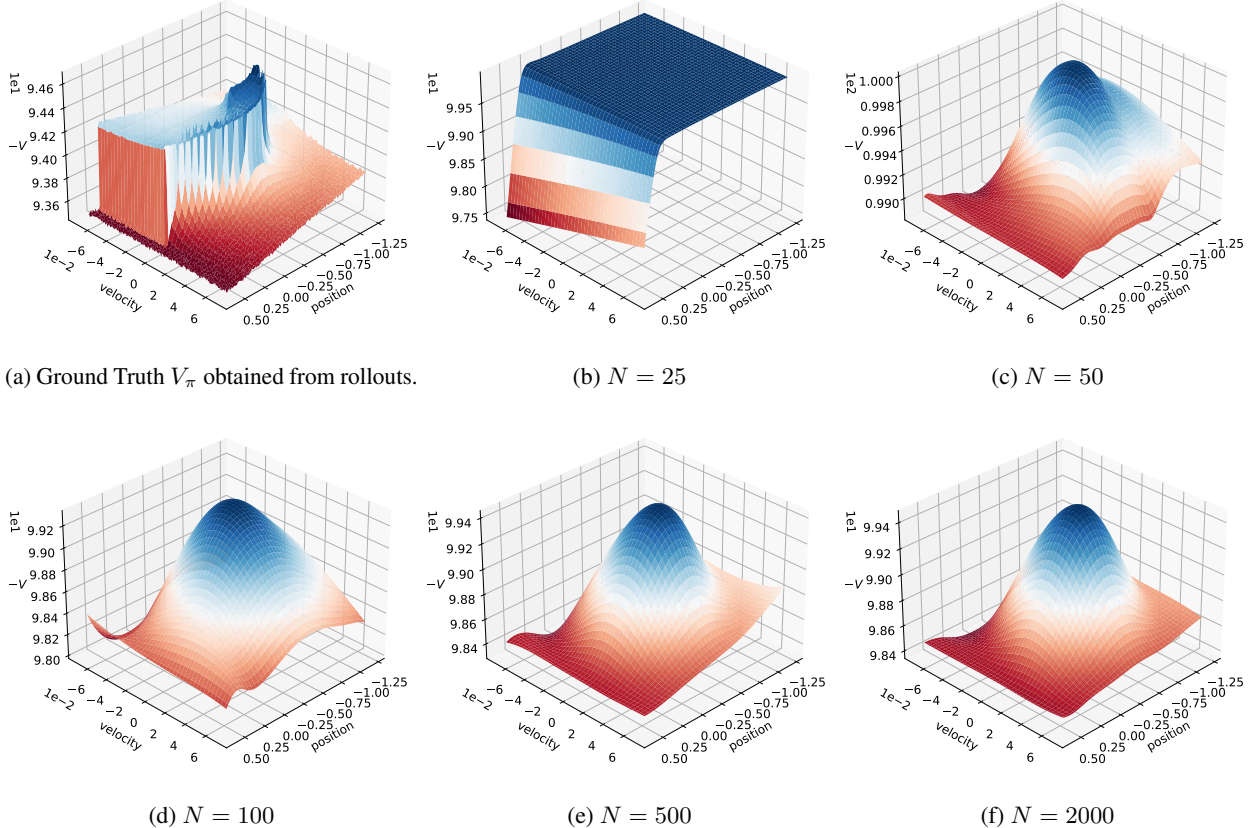


Figure 5: The approximated value function for different batch sizes T with minimal NMSBE, evaluated at the same states as for the MC version.

Results In the following we look separately at training and testing errors and start with the training errors, i.e., the contour plots in the left column of Figure 6. We see that the shapes of isolines for all networks but smallest ones match the shape of the line $N_{\text{net}} \approx N$, which we call *condition line* in the following. We obtain the *condition line* by rounding the amount of parameters N_{net} to the closest value of N and joining those points. The shape implies that the area with same training error follows our condition in Equation (42) from our theoretical investigation. When we increase the amount of data we also have to increase the depth or width of an MLP and vice versa to maximise the chance of avoiding suboptimal minima. Between Figures 6a and 6c the shapes of isolines stay consistent and furthermore, the *condition line* is present at roughly the same training error of -4.994 to -4.697 . Exact learning of all samples indicated by training errors close to zero happens only above the solid black line, i.e., whenever the network has more parameters than the number of training samples.

Next, we address the testing error as shown in the right column of Figure 6. For larger MLPs, where the condition $N_{\text{net}} \approx N$ is available for large values of N , we observe that the region with smallest test error extends always to the *condition line*. This happens e.g. for the MLP $\mathcal{F}(2, 15 \times 3, 1)$ at $N = 500$ or for $\mathcal{F}(2, 20 \times 3, 1)$ at $N = 900$. We see that larger MLPs work more predictable where other MLPs are more sensitive to the training set size. In other words, they do not necessarily increase a threshold of required samples for good performance in our experiment. Slightly smaller MLPs need samples in a similar scale as the largest MLPs to achieve the smallest test error. Those MLPs, which one would consider as tiny such as $\mathcal{F}(2, 6 \times 3, 1)$, can also achieve the minimal test error with the same amount of samples. Thus, if for small MLPs the condition $N_{\text{net}} > N$ is far from being realistic, the well-known statement “the more data the better” applies, as we need a factor of 10 more training data than adjustable parameters. In summary, large MLPs concentrate the region with extreme values for the test errors and amplify the effect of the sample size. For $N \rightarrow 50$ the largest architectures produce out of all runs the highest test error. Hence, by shrinking the amount of parameters in an MLP such that $N_{\text{net}} \approx N$ applies again one can reduce the test error without changing the amount of data. If $N \rightarrow 1000$ one has to employ MLPs with a comparable amount of parameters such that the area with smallest test error is present. These MLPs then possess highest generalisation performance out of all architectures.

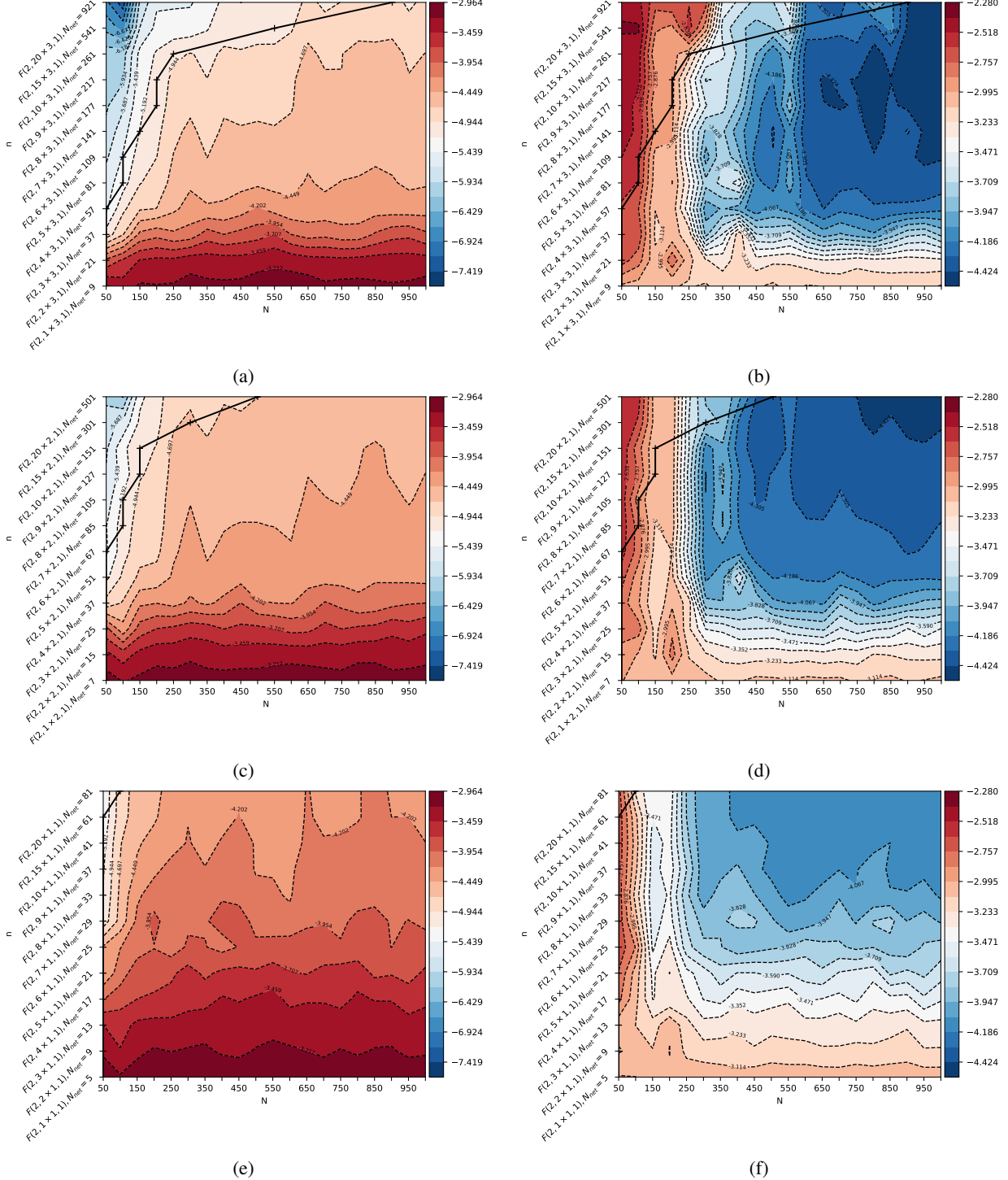


Figure 6: The training and test error of different MLP architectures (vertical axis) for various sample sizes N (horizontal axis). We use a logarithmic scale $Z = \log_{10}(E)$, where E is the original error and Z its plotted value. Red indicates higher errors. In all plots the solid line represents the condition $N_{net} = N$. **Left column:** Training error. **Right column:** Test error.

In training error plots one can see that the shape and position of isolines follows roughly the condition $N_{net} = N$. Lower training error as well as the case of exact fitting happens to the upper left of the black solid line, confirming our considerations from Section 4. The testing error plots reveal that, at least for networks with a large number of parameters, the region with smallest test error reaches close to the condition $N_{net} = N$. However, for all networks the well-known rule “the more data the better” applies, presumably because not all sampled states are far apart.

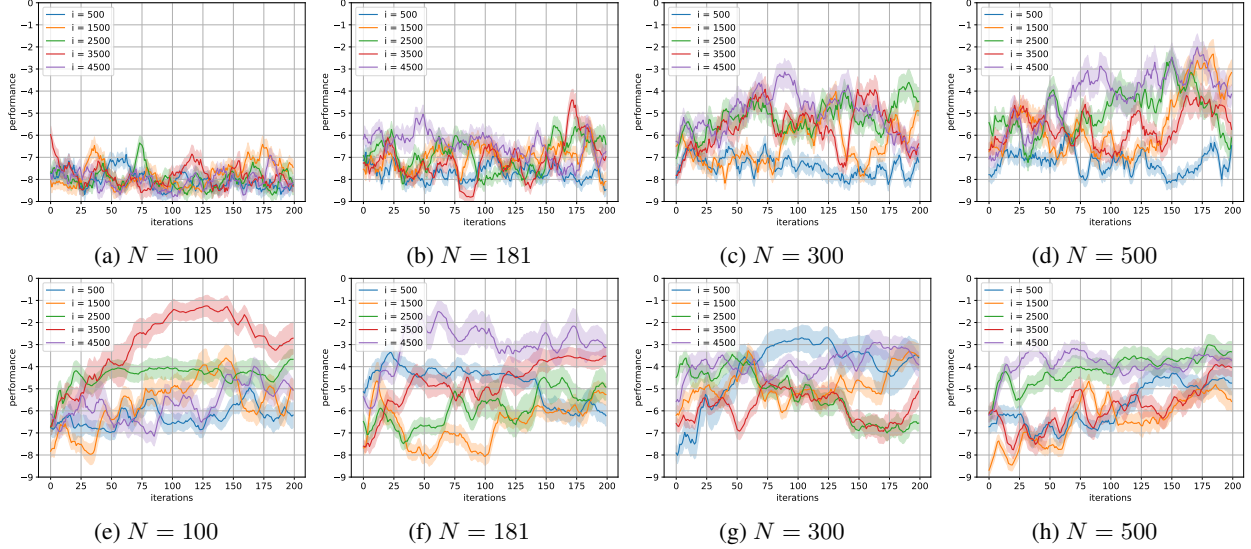


Figure 7: Combining the Residual Gradient Gauss Newton Policy Evaluation with Q-Factors and GIP policies to full Policy Iteration. As environment we use *Cart Pole* and plot the expected reward obtained by performing roll-outs from 5 repetitions. From left to right we vary the number of sampled states. In each Figure the number of Policy Evaluation iterations is changed. In the top row Policy Evaluation starts with a new MLP in every sweep. For the bottom row we reuse the last evaluation of the previous sweep as initialisation for the current one.

Sequentially improving policies are visible, especially when reusing the MLP, however, there is no clear trend for the required number of samples or the optimal amount of Policy Evaluation iterations. Without second order optimisation or when using Semi-Gradients Policy Iteration did not work at all.

6.4 Policy Iteration

Setting For the final experiment we change the environment to *Cart Pole* and test our approach in a Policy Iteration setting. For that purpose we use Q-factors in place of $V_\pi(s)$ and use a greedily induced policy as defined in Equation (7). To represent Q-factors the network input consists of the continuous state and the discrete action index, hence MLPs must have $K + 1$ units in the input layer. More specifically, we use the MLP $\mathcal{F}(5, 10, 10, 1)$ with $N_{\text{net}} = 181$ parameters to approximate the Q-function.

We test different sample sizes $N \in \{100, 181, 300, 500\}$, i.e., the number of states sampled before every Policy Evaluation, and investigate different amounts of policy evaluation steps $i \in \{500, 1500, 2500, 3500, 4500\}$, i.e., the number of descent steps. Finally, we also compare the effect of reusing the last parameters of the previous Policy Evaluation step as initialisation for the current one and refer to this by *transient* and *persistent* as in [Sigaud and Stulp, 2019].

We measure the performance of a policy by performing 10 rollouts with each 500 steps after every improvement step and combine the rollouts as mean, minimal and maximal value. Furthermore, we repeat every experiment 5 times such that we can provide averages of expected returns at each sweep as a summarizing impression of the Policy Iteration processes. Shaded areas represent the mean of all individual spreads of discounted returns. Our results are available in Figure 7.

Results We can only provide results for the Gauss Newton Residual Gradient formulation. Other experiments either diverged (Semi-Gradient) or did not show improving policies over time (first order Residual Gradient). Thus, this experiment already implies that second order information is essential to enable and stabilise Policy Iteration in continuous problems. It also shows that in order to get the benefits of second order approaches, the TD target *cannot* be ignored during the computation of differential maps.

Sequentially improving policies are visible in most plots. Starting with a fresh MLP for each evaluation increases the number of sample states to see a more pronounced improvement over time. When using persistent evaluations, i.e., reusing the MLP parameters corresponding to the last policy, clear improvements are visible also for small sample sizes. Furthermore, the maximum achieved performance is higher than for transient sweeps.

In all graphs of Figure 7 it is hard to find a clear trend for the required number of samples or the optimal amount of Policy Evaluation iterations. As an example, in Figure 7d both $i = 1500$ and $i = 4500$ have a similar high performance around sweep 175. In Figure 7e, using only $N = 100$ samples result for $i = 3500$ reliably in significant better performing policies than when increasing the amount of Policy Evaluation steps to $i = 4500$.

The fact that for $N = 181 = N_{net}$ samples and when using persistent evaluations of policies all repetitions of the experiment come up with good performing policies for the largest amount of Policy Evaluation steps is worth further investigation. But based on our currently available experimental results we cannot make reliable statements at this point. We can only hypothesize why this chaotic behaviour is present. As we are using an approximate Policy Iteration algorithm due to the function approximation, there are two sources of errors: inaccurate Policy Evaluation and erroneous Policy Improvement. First, different than typical settings where samples come from an exploration mechanism, we do select samples uniformly distributed in the whole state space. Thus, our optimisation problem does not have a high resolution focused around at the visited parts of the state space but tries to find a global solution, which is obviously a more challenging problem. Second, we make use of discrete actions. This means, we ask a smooth function approximation architecture to model jumps in the value function, which must occur for example around the balancing point of the pole. Thus, our next step for future work is to include continuous action spaces in our analysis.

7 Conclusion

Deep RL with NN-VFA has become in the recent years one of the most powerful RL paradigms in both research and application. Despite the superior performance, its training and convergence analysis remains challenging due to an incomplete theoretical understanding how MLPs affect the common RL setting. In particular, most previous theoretical analysis of this problem approaches the challenge from the perspective of minimising Mean Squared Projected Bellman Error which is incompatible to recent successful applications.

Our work bridges the gap with a concise critical point analysis of the NMSBE when using MLPs. We address both the discrete and continuous state space setting for a Residual Gradient formulation, i.e., using the *complete* gradient of the NMSBE. We derive conditions on MLPs to ensure a proper behaviour of the optimisation procedure. Over-parametrisation of the MLP is required next to some design principles for MLPs to eliminate suboptimal local minima. Furthermore, full rankness of the differential maps of the MLP enable pleasing convergence properties of gradient descent algorithms. Our analysis unveils the possibility to utilise approximated second order information of the cost function, resulting in an efficient Approximate Newton's method. As part of our work, we also see, why Multi-step Lookahead can help Semi-Gradient algorithms. As the MLP in the TD target gets multiplied with the discount factor with larger powers the effect of ignoring the dependency vanishes naturally.

In several experiments we investigate empirically the minimisation of the NMSBE using a Gauss Newton Residual Gradient algorithm. First, we ensure the correctness of the approximated Hessian close to critical points by demonstrating quadratic convergence on an adapted version of Baird's *Seven State Star Problem*.

Next, in continuous state space problems, we provide consistent and stable convergence properties of Residual Gradient algorithms combined with second order information for a wide range of learning rates. Semi-Gradient algorithms are observed to diverge except for some learning rates. Carefully selecting the learning rate is thus important. First order only Residual Gradients are shown to converge slowly, confirming the known behaviour which explains their unpopularity. Using an approximated Hessian can solve these issues and is essential to develop stable and efficient RL algorithms, which also achieve better final errors. Our experiments also serve as proof of concept that with modern computer systems second order optimisation *is* a possible approach in Reinforcement Learning applications.

Furthermore, we investigate the generalisation capabilities of MLPs when training with approximated second order Residual Gradient algorithms. Training and test errors follow our theoretical insights, meaning that the number of parameters should be synchronised with the number of training samples. We find that deeper architectures do not necessarily increase the number of samples required for good performance, they rather amplify the extreme cases for errors.

Finally, we demonstrate that the application of Residual Gradient methods can work in a full Policy Iteration setting. A well performing policy can be learned by alternating between Policy Evaluation and Policy Improvement, starting from a random initial one. However, our empirical findings did not reveal trends on the number of samples or Policy Evaluation steps needed. Our hypothesis is that the discrete action space stands in conflict with the capabilities of a smooth function approximators such as MLPs. Solving the RL task involves representing jumps in the value function, which might not be possible. Hence, including a continuous action space in our analysis is an important next step for our future work.

In conclusion, considering derivatives of the TD target as done in Residual Gradient algorithms allows us to perform a sophisticated analysis and also provides the foundation for reliable RL algorithms.

Acknowledgements

Supported by Deutsche Forschungsgemeinschaft (DFG) through TUM International Graduate School of Science and Engineering (IGSSE), GSC 81.

References

P. A. Absil, R. Mahony, and R. Sepulchre. *Optimization Algorithms on Matrix Manifolds*. Princeton University Press, 2008.

L. C. Baird III. Residual algorithms: Reinforcement learning with function approximation. In *Proceeding of the 12th International Conference on Machine Learning*, pages 30–37, 1995.

L. C. Baird III and A. W. Moore. Gradient descent for general reinforcement learning. In *Advances in neural information processing systems*, pages 968–974, 1999.

A. G. Barto, R. S. Sutton, and C. W. Anderson. Neuronlike adaptive elements that can solve difficult learning control problems. *IEEE Transactions on Systems, Man, and Cybernetics*, SMC-13(5):834–846, 1983.

D. P. Bertsekas. *Dynamic Programming and Optimal Control: Approximate Dynamic Programming*, volume 2. Athena Scientific, 4th edition, 2012.

D. P. Bertsekas and J. Tsitsiklis. *Neuro-Dynamic Programming*. Athena Scientific, 1996.

D. P. Bertsekas, V. Borkar, and A. Nedić. Improved temporal difference methods with linear function approximation. In *Learning and Approximate Dynamic Programming*, pages 231–235. IEEE Press, 2004.

N. Bhat, V. F. Farias, and C. C. Moallemi. Non-parametric approximate dynamic programming via the kernel method. In P. Bartlett, F. C. N. Pereira, C. J. C. Burges, L. Bottou, and K. Q. Weinberger, editors, *Advances in Neural Information Processing Systems 25*, pages 386–394. The MIT Press, 2012.

W. Böhmer, S. Grünewälder, Y. Shen, M. Musial, and K. Obermayer. Construction of approximation spaces for reinforcement learning. *Journal of Machine Learning Research*, 14(1):2067–2118, 2013.

G. Brockman, V. Cheung, L. Pettersson, J. Schneider, J. Schulman, J. Tang, and W. Zaremba. Openai gym. *CoRR*, abs/1606.01540, 2016. URL <http://arxiv.org/abs/1606.01540>.

Q. Cai, Z. Yang, J. D. Lee, and Z. Wang. Neural temporal-difference learning converges to global optima. *CoRR*, abs/1905.10027, 2019. URL <http://arxiv.org/abs/1905.10027>.

J. Fu, A. Kumar, M. Soh, and S. Levine. Diagnosing bottlenecks in deep q-learning algorithms. In *Proceedings of the 36th International Conference on Machine Learning*, volume 97, pages 2021–2030, 2019.

M. Geist and O. Pietquin. Algorithmic survey of parametric value function approximations. *IEEE Transactions on Neural Networks and Learning Systems*, 24(6):845–867, 2013.

S. Gronauer and M. Gottwald. The successful ingredients of policy gradient algorithms. In *accepted for publication*, 2021.

O. Güler. *Foundations of Optimization*. Springer, 2010.

B. D. Haeffele and R. Vidal. Global optimality in neural network training. In *Proceedings of the IEEE Conference on Computer Vision and Pattern Recognition (CVPR)*, pages 7331 – 7339, 2017.

K. Kawaguchi. Deep learning without poor local minima. In *Advances in Neural Information Processing Systems 29*, pages 586–594, 2016.

S. Lawrence, C. L. Giles, and A. C. Tsoi. Lessons in neural network training: Overfitting may be harder than expected. In *Proceedings of the Fourteenth National Conference on Artificial Intelligence and Ninth Conference on Innovative Applications of Artificial Intelligence*, pages 540–545, 1997.

Y. LeCun, Y. Bengio, and G. Hinton. Deep learning. *Nature*, 521:436–444, 2015.

L.-J. Lin. *Reinforcement Learning for Robots Using Neural Networks*. PhD thesis, Carnegie Mellon University, 1993.

B. Liu, Q. Cai, Z. Yang, and Z. Wang. Neural proximal/trust region policy optimization attains globally optimal policy. *Advances in Neural Information Processing Systems*, 2019.

H. R. Maei, C. Szepesvári, S. Bhatnagar, D. Precup, D. Silver, and R. S. Sutton. Convergent temporal-difference learning with arbitrary smooth function approximation. In *Advances in Neural Information Processing Systems 22*, pages 1204–1212, 2009.

V. Mnih, K. Kavukcuoglu, D. Silver, A. A. Rusu, J. Veness, M. G. Bellemare, A. Graves, M. Riedmiller, A. K. Fidjeland, G. Ostrovski, S. Petersen, C. Beattie, A. Sadik, I. Antonoglou, H. King, D. Kumaran, D. Wierstra, S. Legg, and D. Hassabis. Human-level control through deep reinforcement learning. *Nature*, 518:529–533, 2015.

A. W. Moore. Efficient memory-based learning for robot control. Technical Report UCAM-CL-TR-209, University of Cambridge, Computer Laboratory, 1990.

A. Nedić and D. P. Bertsekas. Least squares policy evaluation algorithms with linear function approximation. *Discrete Event Dynamic Systems: Theory and Applications*, 13(1-2):79–110, 2003.

B. Neyshabur, S. Bhojanapalli, D. McAllester, and N. Srebro. Exploring generalization in deep learning. In *Advances in Neural Information Processing Systems 30*, pages 5947–5956, 2017.

Q. Nguyen and M. Hein. The loss surface of deep and wide neural networks. In *Proceedings of the 34th International Conference on Machine Learning*, 2017.

R. Parr, C. Painter-Wakefield, L. Li, and M. Littman. Analyzing feature generation for value-function approximation. In *Proceedings of the 24th international conference on Machine learning*, pages 1–8, 2007.

R. Parr, L. Li, G. Taylor, C. Painter-Wakefield, and M. L. Littman. An analysis of linear models, linear value-function approximation, and feature selection for reinforcement learning. In *Proceedings of the 25th international conference on Machine learning*, pages 752–759, 2008.

M. Riedmiller. Neural fitted q iteration – first experiences with a data efficient neural reinforcement learning method. In *Proceedings of the 16th European Conference on Machine Learning*, pages 317–328, 2005.

E. Saleh and N. Jiang. Deterministic bellman residual minimization. In *Optimization Foundations for Reinforcement Learning Workshop*, 2019.

J. Schulman, P. Moritz, S. Levine, M. I. Jordan, and P. Abbeel. High-dimensional continuous control using generalized advantage estimation. In *4th International Conference on Learning Representations*, 2016.

J. Schulman, F. Wolski, P. Dhariwal, A. Radford, and O. Klimov. Proximal policy optimization algorithms. *CoRR*, abs/1707.06347, 2017. URL <http://arxiv.org/abs/1707.06347>.

J. V. Shah and C. S. Poon. Linear independence of internal representations in multilayer perceptrons. *IEEE Transactions on Neural Networks*, 10(1):10–18, 1999.

H. Shen. A differential topological view of challenges in learning with feedforward neural networks. *CoRR*, abs/1811.10304, 2018a. URL <http://arxiv.org/abs/1811.10304>.

H. Shen. Towards a mathematical understanding of the difficulty in learning with feedforward neural networks. In *Proceedings of the IEEE Conference on Computer Vision and Pattern Recognition (CVPR)*, 2018b.

H. Shen and M. Gottwald. Demystification of flat minima and generalisability of deep neural networks. In *Workshop on Understanding and Improving Generalization in Deep Learning*, 2019.

O. Sigaud and F. Stulp. Policy search in continuous action domains: An overview. *Neural Networks*, 113:28–40, 2019.

D. Silver. Gradient temporal difference networks. In *Proceedings of the 10th European Workshop on Reinforcement Learning*, volume 24, pages 117–130, 2013.

D. Silver, A. Huang, C. J. Maddison, A. Guez, L. Sifre, G. van den Driessche, J. Schrittwieser, I. Antonoglou, V. Panneershelvam, M. Lanctot, S. Dieleman, D. Grewe, J. Nham, N. Kalchbrenner, I. Sutskever, T. Lillicrap, M. Leach, K. Kavukcuoglu, T. Graepel, and D. Hassabis. Mastering the game of Go with deep neural networks and tree search. *Nature*, 529:484–489, 2016.

D. Silver, J. Schrittwieser, K. Simonyan, I. Antonoglou, A. Huang, A. Guez, T. Hubert, L. Baker, M. Lai, A. Bolton, Y. Chen, T. Lillicrap, F. Hui, L. Sifre, G. van den Driessche, T. Graepel, and D. Hassabis. Mastering the game of Go with deep neural networks and tree search. *Nature*, 550:354–359, 2017.

R. S. Sutton and A. G. Barto. *Reinforcement learning: An introduction*. The MIT Press, 2nd edition, 2020.

R. S. Sutton, C. Szepesvári, and H. R. Maei. A convergent $O(n)$ algorithm for off-policy temporal-difference learning with linear function approximations. In *Advances in Neural Information Processing Systems 21*, volume 21, pages 1609–1616, 2008.

R. S. Sutton, H. R. Maei, D. Precup, S. Bhatnagar, D. Silver, C. Szepesvári, and E. Wiewiora. Fast gradient-descent methods for temporal-difference learning with linear function approximation. In *Proceedings of the 26th International Conference on Machine Learning (ICML)*, pages 993–1000, 2009.

G. Taylor and R. Parr. Kernelized value function approximation for reinforcement learning. In *Proceedings of the 26th International Conference on Machine Learning (ICML)*, pages 1017–1024, 2009.

H. van Hasselt, A. Guez, and D. Silver. Deep reinforcement learning with double Q-learning. In *Proceedings of the AAAI Conference on Artificial Intelligence*, volume 30, pages 2094–2100, 2016.

X. Xu, D. Hu, and X. Lu. Kernel-based least squares policy iteration for reinforcement learning. *IEEE Transactions on Neural Networks*, 18(4):973–992, 2007.

D. Yu and L. Deng. *Automatic Speech Recognition: A Deep Learning Approach*. Springer-Verlag, London, 2015.

C. Yun, S. Sra, and A. Jadbabaie. Global optimality conditions for deep neural networks. In *The 6th International Conference on Learning Representations*, 2018.

C. Zhang, S. Bengio, M. Hardt, B. Recht, and O. Vinyals. Understanding deep learning requires rethinking generalization. In *The 5th International Conference on Learning Representations*, 2017.

S. Zhang, W. Boehmer, and S. Whiteson. Deep residual reinforcement learning. In *Proceedings of the 19th International Conference on Autonomous Agents and MultiAgent Systems*, page 1611–1619, 2020.

A Step by Step Calculations

Differential map of error function For the error function $E: \mathbb{R}^K \rightarrow \mathbb{R}$ and some $F \in \mathbb{R}^K$ we have

$$\begin{aligned}
 E(F) &= \frac{1}{2} (F - P_\pi(R + \gamma F))^\top \Xi(F - P_\pi(R + \gamma F)) \\
 DE(F)[h] &= \frac{1}{2} \frac{d}{dt} \Big|_{t=0} \left[\left((F + th) - P_\pi(R + \gamma(F + th)) \right)^\top \Xi \left((F + th) - P_\pi(R + \gamma(F + th)) \right) \right] \\
 &= \frac{1}{2} \left[(h - P_\pi \gamma h)^\top \Xi \left((F + th) - P_\pi(R + \gamma(F + th)) \right) \right. \\
 &\quad \left. + \left((F + th) - P_\pi(R + \gamma(F + th)) \right)^\top \Xi \left(h - P_\pi \gamma h \right) \right]_{t=0} \\
 &= \frac{1}{2} \left[(h - P_\pi \gamma h)^\top \Xi \left(F - P_\pi(R + \gamma F) \right) + (F - P_\pi(R + \gamma F))^\top \Xi \left(h - P_\pi \gamma h \right) \right] \\
 &= (F - P_\pi(R + \gamma F))^\top \Xi(I_K - \gamma P_\pi)h.
 \end{aligned}$$

Thus, according to Riesz, the gradient is

$$\nabla_F E(F) = \left((F - P_\pi(R + \gamma F))^\top \Xi(I_K - \gamma P_\pi) \right)^\top,$$

Differential map of MLP Consider an MLP $f \in \mathcal{F}(n_0, n_1, \dots, n_{L-1}, n_L)$ and an input $s \in \mathcal{S}$. To calculate the differential map of f for s at the point $\mathbf{W} \in \mathcal{W}$ and a direction $\mathbf{H} \in \mathcal{W}$ first start with a single layer l of the MLP. We have

$$D_{W_l} f(\mathbf{W}, s)[H_l] = D_2 \Lambda_L(W_L, \phi_{L-1}) \circ \dots \circ D_2 \Lambda_{l+1}(W_{l+1}, \phi_l) \circ D_1 \Lambda_l(W_l, \phi_{l-1})[H_l],$$

where $D_1 \Lambda_l(W_l, \phi_{l-1})[H_l]$ and $D_2 \Lambda_l(W_l, \phi_{l-1})[h_{l-1}]$ refer to the derivative of layer mapping Λ_l with respect to the first and the second argument, respectively. For the layer definition in Equation (17) we obtain

$$\begin{aligned}
 D_1 \Lambda_l(W_l, \phi_{l-1})[H_l] &= \frac{d}{dt} \Big|_{t=0} \left[\begin{array}{c} \vdots \\ \sigma \left((W_{l,k} + t \cdot H_{l,k})^\top \cdot \begin{bmatrix} \phi_{l-1} \\ 1 \end{bmatrix} \right) \\ \vdots \end{array} \right] = \left[\begin{array}{c} \vdots \\ \sigma'(\dots) H_{l,k}^\top \begin{bmatrix} \phi_{l-1} \\ 1 \end{bmatrix} \\ \vdots \end{array} \right]_{t=0} \\
 &= \text{diag}(\phi'_l) H_l^\top \begin{bmatrix} \phi_{l-1} \\ 1 \end{bmatrix} =: \Sigma_l \cdot H_l^\top \cdot \tilde{\phi}_{l-1} \\
 D_2 \Lambda_l(W_l, \phi_{l-1})[h_{l-1}] &= \frac{d}{dt} \Big|_{t=0} \left[\begin{array}{c} \vdots \\ \sigma \left(W_{l,k}^\top \cdot \left(\begin{bmatrix} \phi_{l-1} \\ 1 \end{bmatrix} + t \cdot \begin{bmatrix} h_{l-1} \\ 0 \end{bmatrix} \right) \right) \\ \vdots \end{array} \right] = \left[\begin{array}{c} \vdots \\ \sigma'(\dots) W_{l,k}^\top \begin{bmatrix} h_{l-1} \\ 0 \end{bmatrix} \\ \vdots \end{array} \right]_{t=0} \\
 &= \text{diag}(\phi'_l) W_l^\top \begin{bmatrix} h_{l-1} \\ 0 \end{bmatrix} =: \Sigma_l \cdot \bar{W}_l^\top \cdot h_{l-1}
 \end{aligned}$$

where $\Sigma_l \in \mathbb{R}^{n_l \times n_l}$ is a diagonal matrix with its entries being the derivatives of the activation function with respect to the input, i.e., ϕ'_l containing $\sigma'(\dots)$ for all units in layer l . The input to ϕ'_l is the unmodified output ϕ_{l-1} of the truncated MLP. By writing \bar{W} we indicate that the last row is cut off due to the multiplication by zero and $\tilde{\phi}$ shows that the layer output is extended with an additional 1. This resembles homogenous coordinates as they are used with the special Euclidean group $SE(3)$ for computer vision applications. Inserting these parts yields for the differential map

$$D_{W_l} f(\mathbf{W}, s)[H_l] = \Sigma_L \bar{W}_L^\top \cdot \Sigma_{L-1} \bar{W}_{L-1}^\top \cdots \Sigma_{l+1} \bar{W}_{l+1}^\top \cdot \Sigma_l H_l^\top \tilde{\phi}_{l-1}.$$

To shorten this expression let us construct a sequence of matrices for all $l = L-1, \dots, 1$ as

$$\psi_l := \Sigma_l \bar{W}_{l+1} \psi_{l+1} \in \mathbb{R}^{n_l \times n_L},$$

with $\psi_L \equiv 1$, due to the activation function in the last layer being the identity function. Now we can write compactly

$$D_{W_l} f(\mathbf{W}, s)[H_l] = \Psi_l^\top H_l^\top \phi_{l-1}.$$

To arrive at the expression shown in the paper consider a matrix $A \in \mathbb{R}^{n \times m}$ and a compatible column vector $b \in \mathbb{R}^{n \times 1}$. When denoting by A_1, \dots, A_m the m columns of A one can show by straightforward computation the identity

$$A^\top \cdot b = \begin{bmatrix} A_1^\top b \\ \vdots \\ A_m^\top b \end{bmatrix} = \begin{bmatrix} b^\top A_1 \\ \vdots \\ b^\top A_m \end{bmatrix} = \begin{bmatrix} b^\top & & \\ & \ddots & \\ & & b^\top \end{bmatrix} \begin{bmatrix} A_1 \\ \vdots \\ A_m \end{bmatrix} = (I_{m \times m} \otimes b^\top) \cdot \text{vec}(A).$$

Setting $A = H_l$ and $b = \phi_{l-1}$ we get

$$D_{W_l} f(\mathbf{W}, s)[H_l] = \Psi_l^\top (I_{n_l} \otimes \phi_{l-1}^\top) \text{vec}(H_l).$$

Finally, we can combine the expressions for all layers and produce the full differential map with respect to all parameters

$$D_{\mathbf{W}} f(\mathbf{W}, s)[\mathbf{H}] = \underbrace{\begin{bmatrix} \Psi_1^\top (I_{n_1} \otimes \phi_0) & \dots & \Psi_L^\top (I_{n_L} \otimes \phi_{L-1}) \end{bmatrix}}_{\in \mathbb{R}^{n \times N_{\text{net}}}} \cdot \underbrace{\begin{bmatrix} \text{vec}(H_1) \\ \vdots \\ \text{vec}(H_L) \end{bmatrix}}_{\in \mathbb{R}^{N_{\text{net}} \times 1}},$$

where the MLP input ϕ_0 is just the input s . For the application in our work we always have $n_L = 1$ because the value function maps to a scalar value. Using all N inputs at once we arrive at the expression $G(\mathbf{W}) \in \mathbb{R}^{N \cdot n_L \times N_{\text{net}}}$ as shown in Equation (26)

$$D_{\mathbf{W}} F(\mathbf{W})[\mathbf{H}] = \underbrace{\begin{bmatrix} \Psi_1^\top \left(I_{n_1} \otimes \phi_0^{(1)\top} \right) & \dots & \Psi_L^\top \left(I_{n_L} \otimes \phi_{L-1}^{(1)\top} \right) \\ \vdots & \ddots & \vdots \\ \Psi_1^\top \left(I_{n_1} \otimes \phi_0^{(N)\top} \right) & \dots & \Psi_L^\top \left(I_{n_L} \otimes \phi_{L-1}^{(N)\top} \right) \end{bmatrix}}_{=:G(\mathbf{W}) \in \mathbb{R}^{N \cdot n_L \times N_{\text{net}}}} \cdot \begin{bmatrix} \text{vec}(H_1) \\ \vdots \\ \text{vec}(H_L) \end{bmatrix}.$$

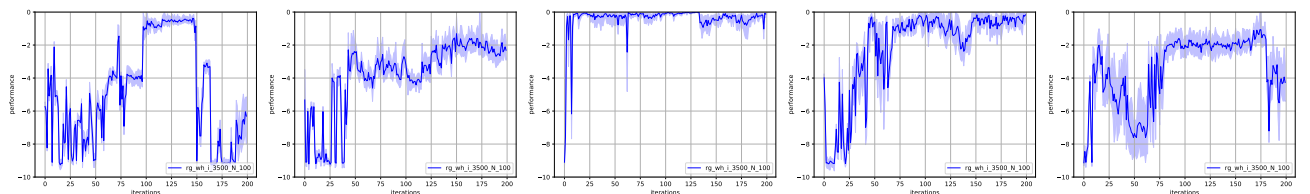
The superscript $(\cdot)^{(i)}$ indicates that the the layer outputs ϕ_l arise from the i -th state in the input layer. Equation (39) originates directly from the difference of $G(\mathbf{W})$ and $G'(\mathbf{W})$

$$\begin{aligned} \tilde{G}(\mathbf{W}) &= G(\mathbf{W}) - \gamma G'(\mathbf{W}) \\ &= \begin{bmatrix} \Psi_1^\top \left(I_{n_1} \otimes \phi_0^{(1)\top} \right) & \Psi_L^\top \left(I_{n_L} \otimes \phi_{L-1}^{(1)\top} \right) \\ \Psi_1^\top \left(I_{n_1} \otimes \phi_0^{(N)\top} \right) & \Psi_L^\top \left(I_{n_L} \otimes \phi_{L-1}^{(N)\top} \right) \end{bmatrix} - \gamma \begin{bmatrix} \Psi_1^\top \left(I_{n_1} \otimes \phi_0'^{(1)\top} \right) & \Psi_L^\top \left(I_{n_L} \otimes \phi_{L-1}'^{(1)\top} \right) \\ \Psi_1^\top \left(I_{n_1} \otimes \phi_0'^{(N)\top} \right) & \Psi_L^\top \left(I_{n_L} \otimes \phi_{L-1}'^{(N)\top} \right) \end{bmatrix} \\ &= \begin{bmatrix} \Psi_1^\top \left(I_{n_1} \otimes \left(\phi_0^{(1)} - \gamma \phi_0'^{(1)} \right)^\top \right) & \dots & \Psi_L^\top \left(I_{n_L} \otimes \left(\phi_{L-1}^{(1)} - \gamma \phi_{L-1}'^{(1)} \right)^\top \right) \\ \vdots & \ddots & \vdots \\ \Psi_1^\top \left(I_{n_1} \otimes \left(\phi_0^{(N)} - \gamma \phi_0'^{(N)} \right)^\top \right) & \dots & \Psi_L^\top \left(I_{n_L} \otimes \left(\phi_{L-1}^{(N)} - \gamma \phi_{L-1}'^{(N)} \right)^\top \right) \end{bmatrix} \end{aligned}$$

as the Kronecker product is bilinear with respect to matrix addition.

B Raw Data

To emphasize the difficulty in visualising the results of our Policy Iteration experiment please take a look at the output of all five individual repetitions for $N = 100$ samples with $i = 3500$ Policy Evaluations steps when using the persistent setting.



While all repetitions of the roll-outs produce repeatedly similar discounted returns, running again the whole experiment produces varying performance curves. By averaging these curves we can highlight the trend in the experiment and produce the plots from Figure 7.